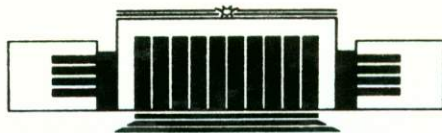




MODERN DEVELOPMENTS IN NUCLEAR PHYSICS

Proceedings of the International symposium on
Modern Developments in Nuclear Physics



June 27-July 1, 1987
Novosibirsk, USSR

Symposium Sponsored by
European Physical Society
U.S.S.R. Academy of Sciences

Editor
O.P. Sushkov

World Scientific

Proceedings of the International symposium on
Modern Developments in Nuclear Physics

MODERN DEVELOPMENTS IN NUCLEAR PHYSICS

June 27-July 1, 1987
Novosibirsk, USSR

Symposium Sponsored by
European Physical Society
U.S.S.R. Academy of Sciences

Editor

O.P. Sushkov

A.N. Skr...
V.G. Tol...
V.F. D...
O.P. Sushkov

 **World Scientific**
Singapore • New Jersey • Hong Kong

EXPERIMENTS WITH AN INTERNAL TARGET
IN THE ELECTRON STORAGE RING

S.G. Popov

Institute of Nuclear Physics
630090, Novosibirsk, U S S R

Introduction

There is no need for proving nowadays the especial value of experiments with electromagnetic probes at various energies and momentum transfers for nuclear physics as well as for elementary particle physics and high energy physics. Well developed theoretical description of the interaction, pointlike character of the probe particle, weak perturbation of the target- all these features are characteristic of an ideal probe of nuclear matter. On the other hand, typical cross sections are small and there exist a "radiative tail" in electron reactions. Besides, to achieve the required accuracy one need high statistics of data. It imposes stringent requirements on experimental facilities, i.e. accelerators, targets, detectors. Due to the mentioned difficulties, almost all experiments with electrons has been, up to recent years, inclusive, with exception of some experiments with predictable kinematics, for example, quasielastic scattering.

Nevertheless, the results obtained in inclusive electron experiments are impressive. In particular, it concerns measurements of the charge density distribution in

elastic electron scattering by nuclei and the transition density in inelastic scattering. As famous example, Fig.1 gives experimental results on the elastic electron scattering by ^{206}Pb and ^{205}Tl nuclei. The accuracy of these measurements turns out to be sufficient to extract the charge density of the 3S proton shell ¹.

However, the modern research deals mostly with more complicated kinematic cases, as well as more complicated physical problems. Thus, the inclusive experiments seem to be insufficiently informative.

Modern experimental program

The interest to exclusive electromagnetic experiments on various nuclei concerns both the wide range of momentum transfers (from some inverse Fermi units to decimal fractions) and transferred energies (excitation energies) up to hundreds of MeV. It is due to the fact that different degrees of freedom of nuclear matter, such as clusters, nucleons, mesons, quarks, are to be studied. To compare physicist's desires with the modern experimental possibilities available, some experimental projects under discussion are evidently worthy to be listed. Some of them can be classified according to different research fields of nuclear matter.

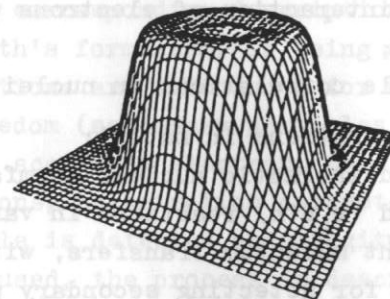
WHAT DO NUCLEI CONSIST OF?

I. Quark nature of nuclear structure:

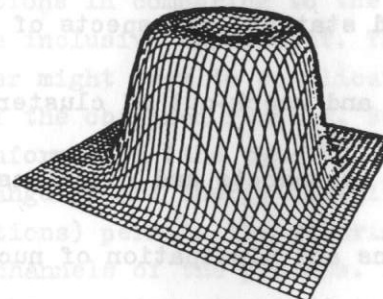
- a) Asymptotical behaviour of the elastic formfactor for few-nucleon systems;
- b) Spectroscopy of nuclei with intrinsically excited nucleons;
- c) EMC-effect ...

II. Contributions of meson exchange currents:

^{206}Pb



^{205}Tl



3S

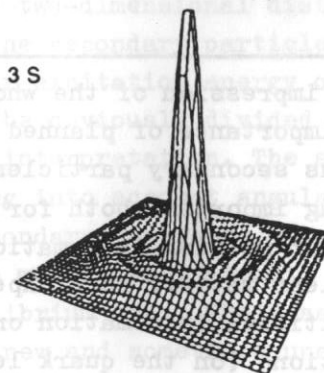


Fig. 1. Charge distributions in the ^{206}Pb and ^{205}Tl nuclei and the 3-S shell proton distribution density (arbitrary units).

- a) Inelastic interaction of electrons with few-nucleon systems;
- b) Two-particle correlations in nuclei ...

III. Nucleon configurations in nuclei:

- a) Elastic and inelastic nuclear formfactors ...
- b) $(e, e'p)$ and $(e, e'n)$ reactions in various nuclei at different momentum transfers, with high energy resolution for detecting secondary particles ...

IV. Collective and statistical aspects of the nuclear dynamics:

- a) Excitation and knock-out of clusters including heavy fragments;
 - b) Collective resonances and rotations;
 - c) Fission;
 - d) Fluctuations and dissipation of nuclear collective motion;
- ...

To get a fuller impression of the whole picture it is worthy to note the importance of planned experiments with production of various secondary particles (for example vector mesons). Being important both for the study of nuclear structure and for getting information on the particle behaviour in nuclear matter, such experiments will supply us with the additional information on the nature of fundamental interactions (on the quark level).

Polarized experiments are destined to separate charge formfactors in nuclei with nonzero spins from multipole ones, to measure the neutron and proton charge structure. It was said at Workshop on the CEBAF research program that "we are about to enter a new era. The era of internal target and polarization phenomena...". It means that one can extract new independent characteristics of structures under study by the coincidence and polarization

experiments. A corresponding description, the so-called super-Rosenbluth's formalism, is being developed². New structure functions are introduced for new experimental degrees of freedom (secondary particles detected in coincidence with a scattered electron, their energy and angular distributions, polarization parameters). When one secondary particle is detected and longitudinally polarized electrons are used, the process is described with five structure functions in comparing to the two functions in the case of the inclusive experiment. The increase of the parameter number might seem to complicate the physical interpretation of the obtained results. But in fact, the new physical information (the type of the secondary particles, their angular and energy distributions, separated structure functions) permits the discrimination of different physical channels of the process. As an example, Fig. 2a shows the two-dimensional distribution of 160 $(e, e'p)$ events. The secondary particle energy is plotted versus the nuclear excitation energy on this map of events which can be obviously divided into 3 groups with a clear physical interpretation. The analysis of these groups with taking into account angular and energy distributions of secondary particles allows to determine physical reaction mechanisms: direct, resonant, statistical and pre-equilibrium ones. Their separate processing provides us with new and sometimes unexpected results³.

The future great progress in the low-, intermediate- and high-energy nuclear physics is connected with putting into operation a new generation of experimental facilities with intense (high luminosity) continuous electron beams and with the possibility to carry out coincidence polarization experiments.

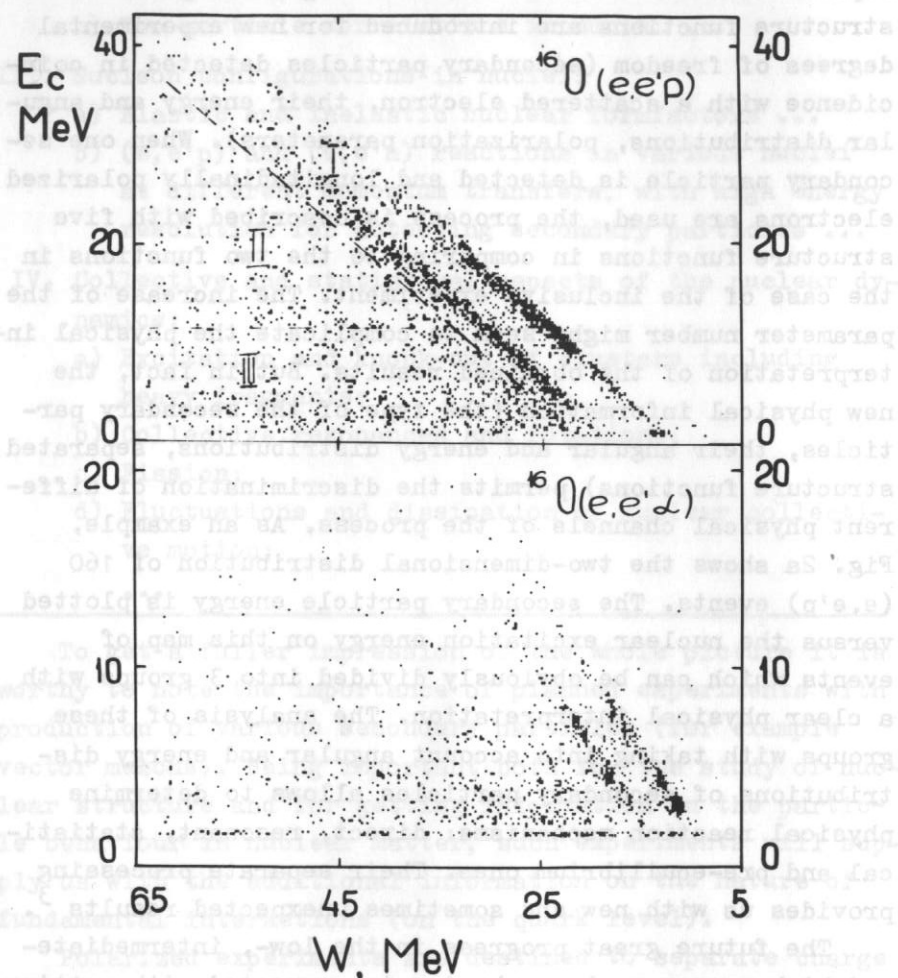


Fig. 2. The distribution of $(e, e'C)$ -like events, where C is a charged particle: proton (a) and α -particle (b). W is the excitation energy of a nucleus (MeV), E_c is the energy of a secondary particle (MeV).

Requirements to modern experimental facilities

The basic requirement to accelerators for experiments with detecting scattered electrons in coincidence with reaction products is the possibility to use a continuous or a quasicontinuous (with the negligible fine time structure) accelerated electron beam. It is necessary for suppressing the accidental coincidence background. Nowadays linear accelerators are most widely used as accelerated electron sources. Their main advantage is the high intensity. But, linear accelerators have, as a rule, the small duty factor, which makes practically impossible their coincidence operation at high intensity.

Recently, the accelerator development had lead to the chance of meeting the demands of the experimental nuclear physics. As a result, there has appeared a great number of electron accelerator projects over a range of energies from tens of MeV to 4 GeV, some of them already being realized (Table I).

TABLE 1

THE CONTINUOUS ELECTRON BEAM FACILITIES

Laboratory	Type of accel.	Energy, MeV	D.F. %	Average curr. mA
Novosibirsk, USSR				
1. VEPP-2	SIT	100-500	90	0.5 A
2. VEPP-3	SIT	400-2100	100	0.1 A
Stanford, USA				
3. LINAC	RL	70-120	75	20
4. PEP	SIT	2-15GeV	100	50 mA
Illinois, USA				
5. Illinois, USA	RM	100	100	10
Amsterdam, Neth.				
6. Amsterdam, Neth.	LA	500	2.5	20
Saclay, France				
7. Saclay, France	LA	600	1.0	1.0
Mainz, FRG				
8. Mainz, FRG	RM	180	100	30
MIT, USA				
9. MIT, USA	LA	850(1000)	1.0	0.5(85)

10. Tohoku, Japan	ST	150	80	0.5
PROJECTS				
11. Darmstadt, FRG	RL	130	100	20
NBS, USA				
12. RTM-1	RM	185	100	550
13. Lund, Sweden	RM+ST	100-550	100	10
14. Saskatoon, Canada	LA+ST	300	80	30(300mA)
15. Sao Paulo, Brasil	LA+ST	17	100	100
16. Saclay, France	RL	500-3000	100	100
17. Mainz, FRG	RM	840	100	100
18. CEBAF, USA	RL	500-4000	80	240
19. Illinois, USA	RM	450	100	20
20. MIT, USA	RL+ST+SIT	250-1000	100	85(80 mA)
21. Bonn, FRG	ST	3500	60	
22. Mosc. Univ. USSR	RM	110	100	100
23. Kharkov, USSR	LA+ST	2000	100	
24. Novosibirsk, USSR	SIT	100-220	90	1.0 A
25. Tsukuba, Japan	LA	500	2.0	100
26. Amsterdam, Neth.	ST	700	90	100

LA -Linear accelerator; RL -Recirculating linac;
 RM -Racetrack microtron; ST-Stretcher; SIT -Superthin
 internal target.

This table contains essentially 3 types of devices: the continuously operating microtron, the conventional linear accelerator with an additional stretcher set-up, and the electron storage ring with an internal target. The first type has obviously gained a better currency. This is apparently due to the fact that in this case a natural transition occurs from the conventional experimental facilities with linear accelerators preserving the main ideology of experimenting (external targets, spectrometers, secondary particle detectors). These arguments are also applicable to the stretcher-type variant with

the difference, that the electron stretcher is still underdeveloped and is operating now in a single laboratory⁴. The electron emission efficiency is worse than it was expected and insufficient for the high power of the emitted beam.

The Novosibirsk Institute of Nuclear Physics is so far the only laboratory that makes use of an electron storage ring with a superthin internal target for experiments. The advantages of this experimental set up are:

- quasi-continuous regime of operation;
- effective use of the injected beam, that results both in high luminosity of the experiment and in good background conditions;
- possibilities to use unique targets (or beams) and to register slow secondary particles;
- good kinematic experimental conditions at high luminosity⁵.

In this case the technical ways of forming the target and arranging the experimental equipment differ from those traditionally used in the experiments of this kind. That, perhaps, accounts for the fact that, when a laboratory with a developed experimental culture faces the problem of constructing a new type of experimental facility, the variant with an emitted beam seems to be preferable due to the possibility to use the old detectors and to maintain the old experimentalist's psychology. Nevertheless, it should be mentioned, that if the cost of the detectors and the experimentalist's psychology reorganization are not taken into account, the accelerating part with the conventional well known linear low-intensity pulse accelerator plus a specialized storage ring, turns out to be a great deal cheaper in comparing with the high-intensity continuous source of high energy electrons most of them being accelerated only to be shedded

into a special absorber and to worsen the experimental background conditions. Besides, some types of experiments are, no doubt, easier to carry out (or, to be more precise, are more efficient) with the use of internal targets. Such are the experiments with polarized jet targets, experiments that require the registration of slow secondary particles etc. It accounts for the interest to the internal target methodics that has grown up in recent years⁶.

Superthin internal target technique

Internal targets have been long known to be used in accelerators. They were used, in particular, for forming secondary beams emitted from cyclic accelerators. Well known are the experiments on measuring the interference of Coulomb and strong interaction in high energy proton scattering from the hydrogen target⁷. Since a thin target has been used, as it was necessary to register slow recoil protons, the experimental luminosity of the emitted beam has been very low. Placing the target on the closed orbit of an accelerator permits the beam to cross the target repeatedly with gaining the respective increase of luminosity. The crossing multiplicity was limited, as usual, by the time during which the experimental parameters (the energy and the size of the beam, angular and the energy spread) remained satisfactory. The optimal conditions are achieved when the number of crossings is determined by the target thickness (the worsening of the beam parameters is due to the energy losses or to the scattering by the target). This operation regime is called a thin target one.

When using the particle oscillation damping mechanism there appear new possibilities, namely the electron cooling for heavy particles and the synchrotron radiation for electrons. The target thickness in the latter

case should be chosen in such a way that the lifetime of electrons is determined by the target and is longer than the time of the oscillation damping. In this case multiple processes are suppressed and the beam has stable angular and energy spreads. This operating regime is called a superthin target one. The effective target thickness (the product of the thickness by the number of beam crossings before its loss) is independent on the actual target thickness. The diminishing of the target thickness results in the proportional growth of the particle lifetime and, hence, of the number of crossings. In most cases the lifetime of electrons is determined by an energy loss due to the single bremsstrahlung, with the effective target thickness equal to 0.2 rad unit length. Other details of operating with a superthin internal target have been mentioned above. The development of this experimental technique has long been carried out in Novosibirsk⁶, general principles have been stated, proved and utilized in a number of experiments some of them being discussed below.

Nuclear structure studies

Experiments on detecting the electron scattering by a nucleus in coincidence with decay products provide us with unique new possibilities opening a new stage of nuclear research. Experiments of such kind are being carried out already in a number of laboratories of different countries.

As an example, let us discuss an experiment on the ^{16}O using electrons with an energy of 130 MeV scattered at an angle of 51° ³. The energy lost by a scattered electron was measured within a wide range (0-70 MeV). Secondary charged particles were registered in coincidence with the electron, with measuring their energy and the escape angle. The equipment lay-out in the experimental straight

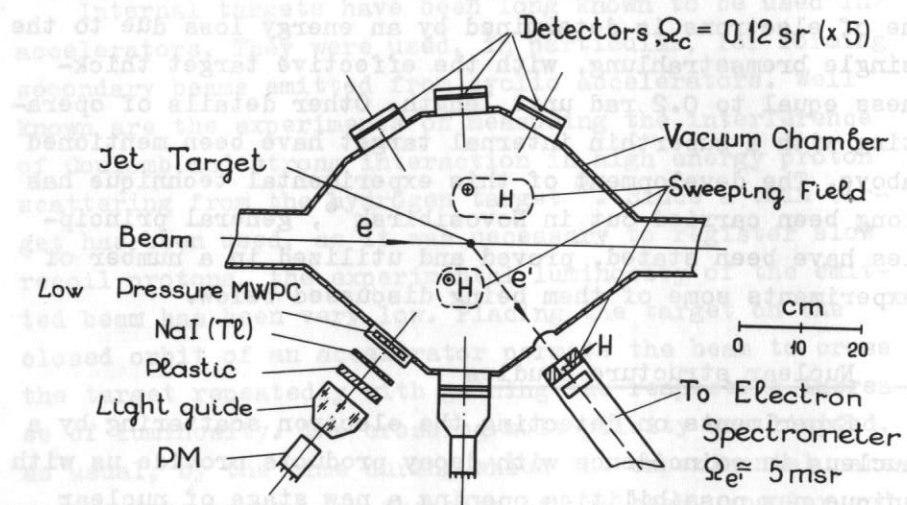


Fig. 3. The experimental lay-out for the nuclear excitation experiments in coincidence with the secondary particle registration.

section is presented in Fig. 3. Fig. 2(a,b) shows the characteristic two-dimensional distributions of a number of events on the plane where axes correspond to the nuclear excitation energy (the energy lost by an electron) and to the secondary particle energy (energy of a proton and of an α -particle, respectively). These distributions are given for a 35° angle for protons and for a 0° angle for α -particles with respect to the direction of the momentum transfer in the scattering plane.

The analysis proton events of considering their angular distributions permits us to separate them into 3 groups: Region I on the event map combines events in the "lines", corresponding to processes when the excitation energy goes to the secondary particle kinetic energy. It means that the residual nucleus remains in a fixed state (the first "line" corresponds to the case, when the residual ^{15}N nucleus remains in its ground state- that is so-called Po-line, etc.). Region III contains events with isotropic angular and Maxwell energy distributions, which are characteristic of statistical equilibrium processes. Region II contains the so-called pre-equilibrium events. For α -particles the situation is similar with the characteristic property, when in the Region I one sees concentration events of on "lines" responsible for the narrow resonances.

As an example of the analysis of events divided in accordance with the mentioned above physical criteria, let us consider the following two figures. In Fig. 4 there the Po-line analysis is presented. The angular distributions Po-line protons were analysed for different excitation energies. In particular, the particle emitting mechanism was assumed to be determined by the direct and resonant processes. The corresponding angular distributions with taking in account their interference was used for fitting.

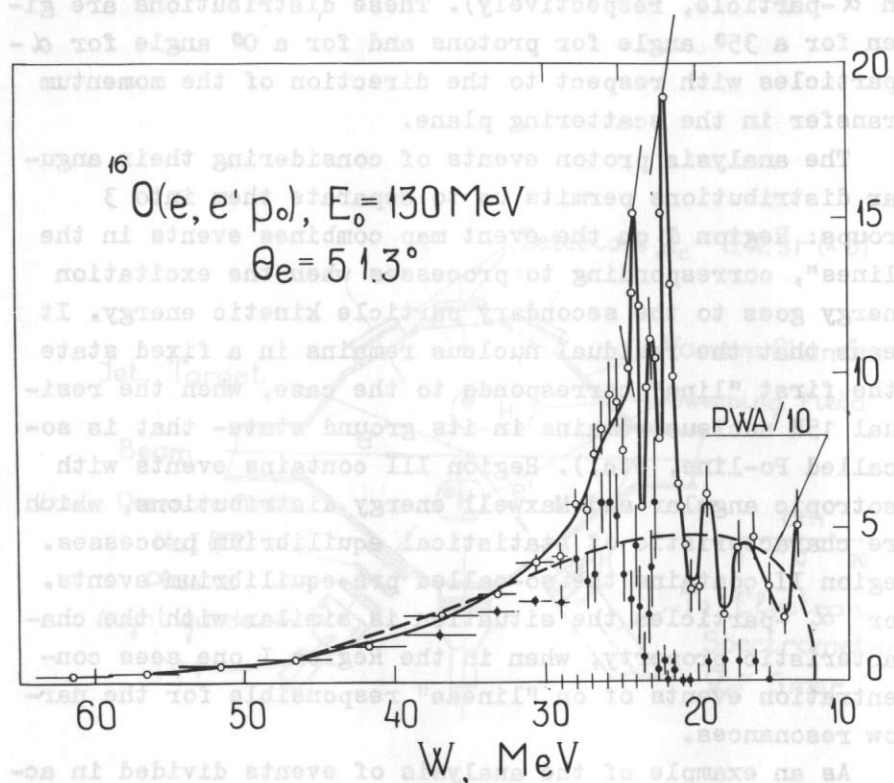


Fig. 4. Total $^{16}\text{O}(e, e'p)$ reaction cross section (circle points) and a part of cross section, determined by a direct process (full points) versus the nucleon excitation energy (MeV).

As a result the total $(e, e'p)$ cross section depending on the excitation energy (circle points) as well as the direct process cross section are shown. The practical disappearance of the direct cross section at excitation energies in the interval from the proton threshold up to 22 MeV seems to be unexpected result.

Fig. 5 shows the temperature dependence on the nuclear excitation energy which is calculated from the Maxwellian energy distribution of "equilibrium" events of the Region III. The assumption of the independence of this temperature on the excitation energy seems preferable in comparison with standard calculations⁸ presented in the figure.

Other examples of the result processing might suggested, that gave on interesting and often unexpected information.

Similar investigations might be of a great interest if carried out on different nuclei at different momentum transfer with detecting charged and neutral secondary particles. In some cases it seems rather perspective to separate response functions - longitudinal and transverse ones and the so-called fifth response function. For this purpose secondary particle detectors are necessary to be located out of the scattering plane and longitudinally polarized electrons should also be used.

Polarization experiments with an internal target

The experiment on separating the charge and the quadrupole deuteron formfactor is one of the most important experiments for studying the nucleon-nucleon interaction. The deuteron is the simplest strongly interacting two-body system which accounts for the longterm interest to its detailed study. The problem consists, to put it roughly, in the necessity for the charge non-sphericity to be

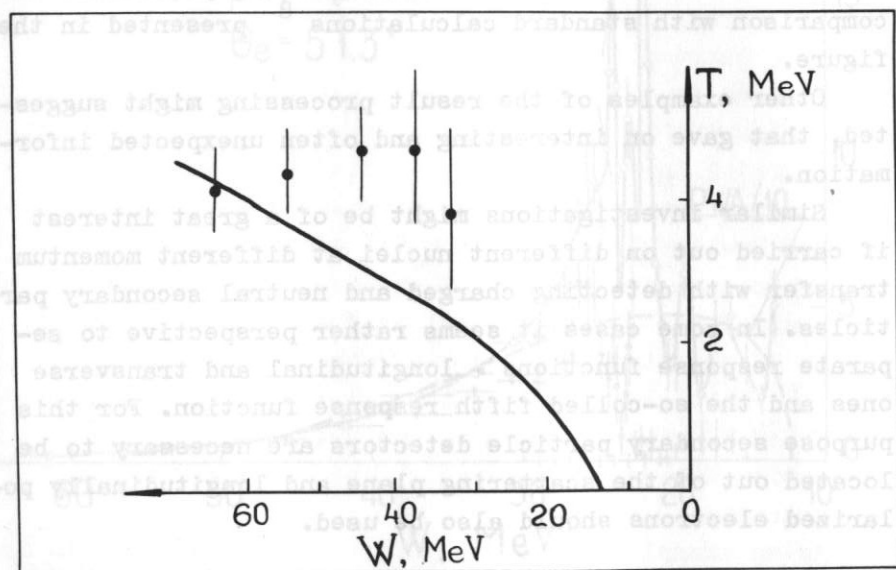


Fig. 5. Temperature dependence T (MeV) of equilibrium protons (region III of Fig. 2a) versus the nucleon excitation energy (MeV). The curve is calculated according to 8.

measured at different distances (at different momentum transfers). In other words, this experiment allows to extract the d-wave fraction of the deuteron wave function, non-centrality of the nucleon-nucleon interaction. It is evident, that these studies are to be carried out by means electron scattering on tensor polarized deuterons, because a non polarized "tumbling" target has a spherically symmetrical averaged charge distribution.

There are two possible variants of planning this experiment. The recoil deuteron polarization can be measured. This way was used in the MIT-SLAC experiment⁹ to demonstrate possibilities of this method. Unfortunately, the progress in this type of experiment at the high momentum transfer (up to five inverse Fermi) is showed down because of sharply worsened possibilities to analyse the recoil deuteron polarization with the energy increasing.

A more evident method and, what is more important, having a better perspective for high momentum transfer is the method of measuring the asymmetry of the elastic electron scattering by a tensor polarized deuteron target. Attempts were made to carry out such an experiment on an external solid cryogen polarized target. But the integral experimental luminosity was too small due to the weak resistance of the target to the beam radiative influence. In particular, using one of the most radiationproof target (ammonia) in the Bonn experiment¹⁰ allows to use the electron current of 0.4 nA only.

It seems that an adequate method consists in the use of a gas polarized jet internal target in a storage ring. The small target thickness is compensated here by a great number of the electron beam crossing. In Novosibirsk in 1985 and 1986 there were performed measurements of the asymmetry in the electron scattering on a polarized deuteron target at the VEPP-2 electron storage ring at energi-

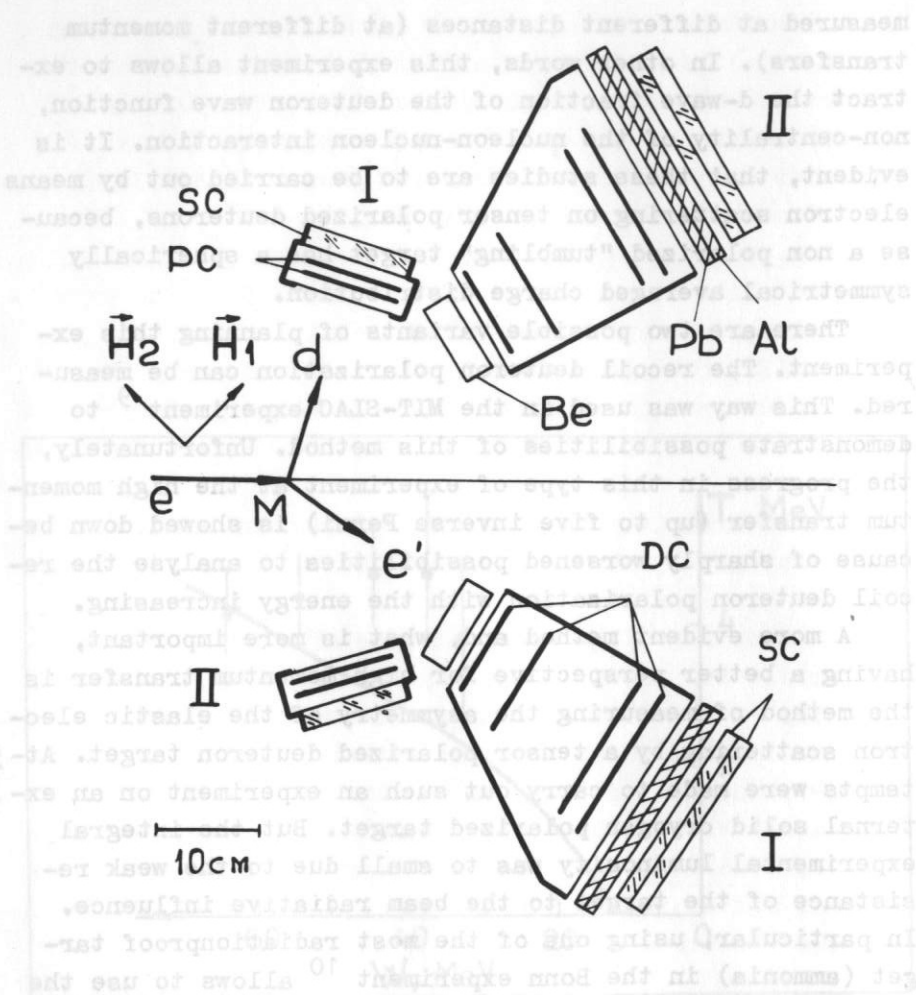


Fig. 6. The scheme of the experimental arrangement with a polarized deuteron target (at the VEPP-2 facility): DC- drift chambers, PC- proportional chambers, SC- scintillation counters, Be, Pb, Al- absorbers, H1(H2)- magnetic field. routing the target polarization.

es of 290 and 400 MeV ¹¹.

Fig. 6 shows the equipment arrangement. Data accumulation is carried out for two momentum transfer directions simultaneously- in parallel and perpendicular directions with respect to the direction of the target polarization. After changing the direction of polarization the detector which have been registered recoil deuterons with one of two possible polarizations registers another one and vice versa. Such a subtraction method of the asymmetry measurements makes it possible to exclude in the first order the effect of the systematical errors connected with detector nonefficiency, different solid angles etc. The results of these measurements are presented in Fig. 7 together with the results obtained in ⁹.

No doubt, the results at higher momentum transfers are of the greatest interest. Experiments of such kind are carried out now in Novosibirsk at the VEPP-3 facility at the electron energy of 2.0 GeV. In Fig. 8 this experiment lay-out is presented. Two pairs of detector sets are used to perform the asymmetry measurements with the help of the subtraction method also. The target jet crosses the electron beam at an angle of 30° to increase the interaction region and, thus, the target thickness. Preliminary results are illustrated in Fig. 7, final ones will be published after accumulating sufficient statistics and its thorough processing.

The registration system makes it possible to perform simultaneous accumulation of information on the deuteron disintegration. In principle, this experiment can us provide with a rich information including also the separation of the charge and quadrupole formfactors. But extracting this information from the experimental data will face great theoretical difficulties because of the necessity to take into account the final state interaction,

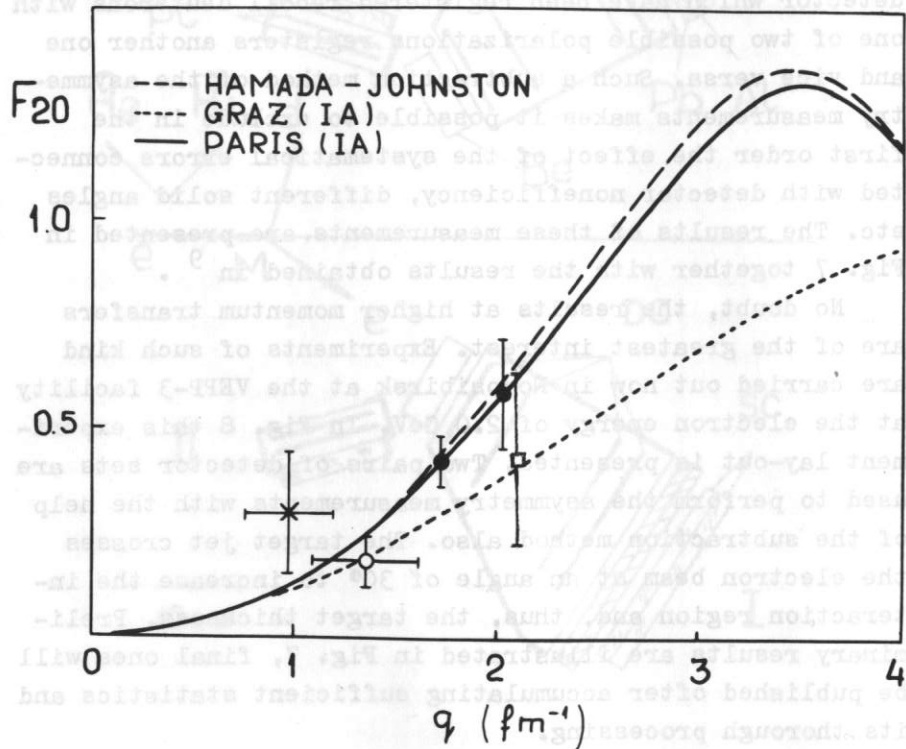


Fig. 7. Analysing power of the F_{20} reaction depending on the momentum transfer. Solid points are taken from 9, the square point is a preliminary result of VEPP-3. Curves correspond to calculations performed with use of various nucleon interaction potentials.

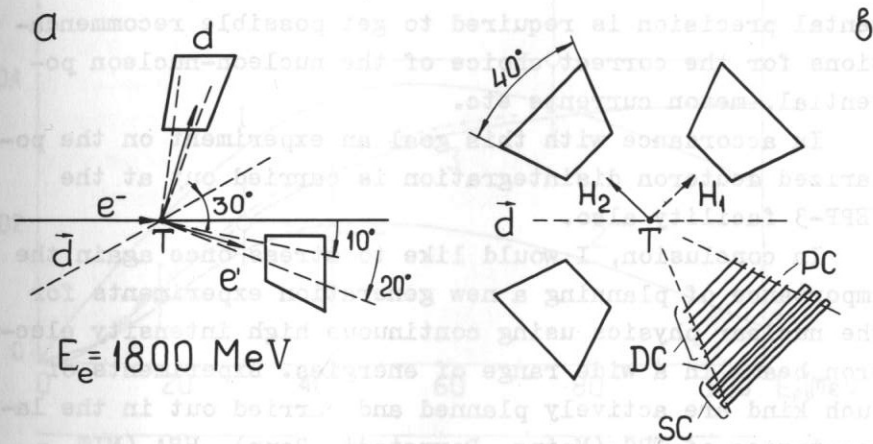


Fig. 8. The scheme of the VEPP-3 experiment with a polarized deuteron target: DC- drift chambers, PC- proportional chambers, SC- scintillation counters, H1(H2)- magnetic field, routing the target polarization.

meson currents contribution, relativistic corrections. Though these contributions are of a great separate interest. Fig. 9 presents the measured asymmetry of the polarized deuteron electrodisintegration versus the transferred energy. The measurements were performed at the VEPP-2 facility at an electron energy of 180 MeV¹². The experimental data contradict both the simplest plane wave and relativistic calculations¹³. There is a good agreement of the experimental results with the Arenhovel calculation within the measurement accuracy¹⁴. A higher experimental precision is required to get possible recommendations for the correct choice of the nucleon-nucleon potential, meson currents etc.

In accordance with this goal an experiment on the polarized deuteron disintegration is carried out at the VEPP-3 facility also.

In conclusion, I would like to stress once again the importance of planning a new generation experiments for the nuclear physics using continuous high intensity electron beams in a wide range of energies. Experiments of such kind are actively planned and carried out in the laboratories of FRG (Mainz, Darmstadt, Bonn), USA (MIT, SLAC, Illinois) France (Saclay), Netherlands NIKHEF), USSR (Novosibirsk). As is seen from the table of facilities this club will soon be joined by a number of powerful laboratories with high-level experimental traditions. The next step will be the wide use in experiments of longitudinally polarized electrons preserving the coincidence registration of reaction products. Mention should also be made of the possible use in these experiments of electron storage rings with a superthin internal target. That provides us with unique possibilities using more economical tools in comparing with conventional ones.

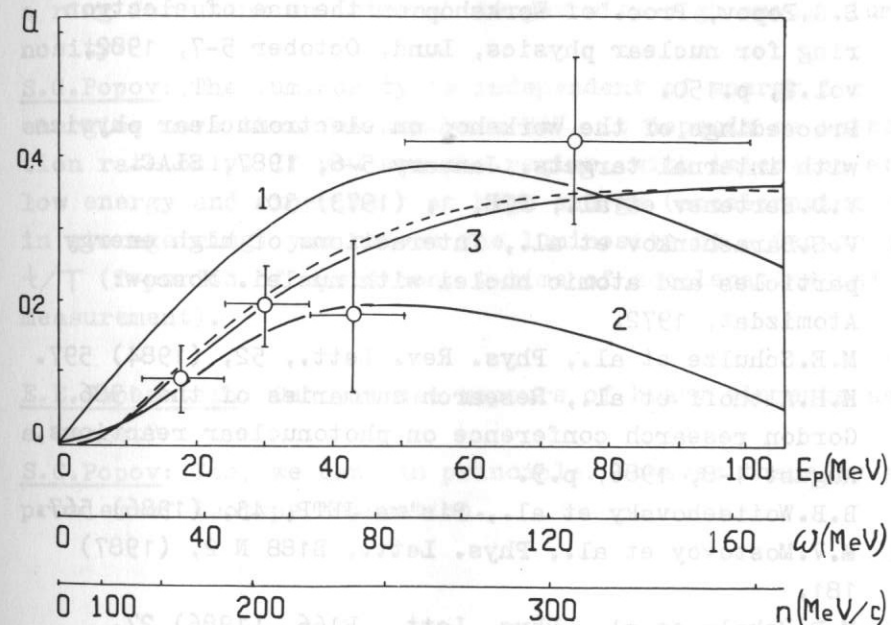


Fig. 9. Electrodisintegration asymmetry for polarized deuterons dependent on the transferred energy (MeV). E_p and n are the proton energy (MeV) and the neutron-spectator momentum (MeV/c). Curve 1 corresponds to the calculation in the plane wave approximation, 2 and 3 are according to 13 and 14 respectively.

References

- 1 B.Frois et al., Nucl. Phys., A396, (1983) 409.
- 2 T.W.Donnelly, 1984 Summer Workshop, June 25-29, 1984 CEBAF, Newport News, p.254.
- 3 V.F.Dmitriev et al., Nucl. Phys., A464, (1987) 237.
- 4 T.Tamae et al., IEEE Trans., NS-30 N 4, (1983) 3235.
- 5 G.I.Budker et al., Yad. Fiz., 6, (1967) 775.
S.G.Popov, Proc. of Workshop on the use of electron ring for nuclear physics, Lund, October 5-7, 1982, vol.2, p.150.
- 6 Proceedings of the workshop on electronuclear physics with internal targets, January 5-8, 1987, SLAC.
- 7 V.D.Bertenev et al., PTE, 1, (1973) 30.
- 8 V.S.Barashenkov et al., Interactions of high energy particles and atomic nuclei with nuclei. Moscow: Atomizdat, 1972.
- 9 M.E.Schulze et al., Phys. Rev. Lett., 52, (1984) 597.
- 10 K.H.Althoff et al., Research summaries of the 1986 Gordon research conference on photonuclear reactions, August 4-8, 1986, p.9.
- 11 B.B.Woitsehovskiy et al., Pis'ma JETP, 43, (1986) 567.
- 12 M.V.Mostovoy et al., Phys. Lett., B188 N 2, (1987) 181.
- 13 M.P.Rekalo et al., Phys. Lett., B166, (1986) 27.
- 14 H.Arenhövel, private communication.

DISCUSSION

R.J.Holt: What steps are you taking to improve the luminosity for the polarization experiments?

S.G.Popov: We are working to rise the polarized target density, the luminosity will grow proportionally.

C.Schuhl: Do you think there is a maximum of energy for a ring for using an internal target with high enough luminosity?

S.G.Popov: The luminosity is independent of energy for energies more than few hundreds MeV. It depends on injection rate only. If you use the regime, with injection at low energy and experiment at high energy (accelerating in storage ring) you reduce the luminosity by a factor t/T (T -period of operation, t -time of accelerating and measurement).

E.E.Sapeshtein: Can you use vapours of heavy elements as a target?

S.G.Popov: Yes, we can, in principle. However there is a problem of isotope separation.

A.Klein: Would you comment on the idea of Barut and Wong of a magnetic resonance which seems to me an attractive idea which one can investigate using quantum electrodynamics?

G.Soff: We investigated the approach of Wong based on idea of Barut to explain the striking peaks in the positron spectra. However, it turned out that this approach displays many deficiencies. First of all, the solutions which were obtained by Wong after performing several approximations are not solutions of the original equation they started from. Secondly, the original equation itself seems to be wrong because it implies a wrong nonrelativistic limit.

A.Klein: I agree that the technical means used so far by Wong are completely unacceptable. Also the Bethe-Salpeter equation is hopeless for this problem; but I believe that something can be done (I have an equation to try).

G.Soff: The solution of the Bethe-Salpeter equation in this respect would be highly desirable. Perhaps more fundamental is an approach of Mathias Graliak in Frankfurt. He tries, starting from the first principles like scale invariance, to prove that no magnetic resonance as proposed by Barut can exist in QED.

V.M.Pugach: You have demonstrated strong dependence of the positron yield on the charge of colliding heavy ions. Is there any dependence on the energy and is there the chance to create strong enough field by lighter ions at higher energies or by powerfull laser? Have you any estimates?

G.Soff: We have made evaluations. There is a threshold for positron production near the Coulomb barrier. The higher energies for other heavy ions are to be still investigated.

QUARK-GLUON PLASMA. THEORY AND EXPERIMENTS

E.V.Shuryak

Institute of Nuclear Physics, Novosibirsk 630090, USSR

1. INTRODUCTION

In this talk I discuss the following topics: (i) recent progress in understanding of the QCD vacuum structure and of the nature of phase transitions, separating ordinary matter from the quark-gluon plasma (QGP); (ii) the role of this transition in the expansion of the "drop" of the quark-gluon plasma, and (iii) the relevant experimental data.

But before I come to physics, let me make some general comments. We witness now strong convergence of nuclear and hadronic physics, and this talk is a good example of it. Sceptics say to this that hadronic physics, now decoupling from the frontier of the highest energies, is going to become "just one more nuclear physics", one more field rich in phenomenology but not strongly related to the fundamental physics. I am the optimist, so I join their opinion that in the foreseeing future both nuclear and hadronic physics be based on the well developed QCD, becoming a kind of "another atomic physics".

Today we have QCD, the fundamental theory of strong interaction, but Lagrangian written on the blackboard is not yet the theory. We have to understand what it really

predicts. Naturally enough, people start with the consideration of the simplest objects. It may appear that the most simple one is the ground state, the QCD vacuum, and next to it are the lowest excitations, say pions and nucleons. However, whatever important these objects are, they are by no way simple. It sounds like a paradox, but highly excited hadronic matter in the "quark-gluon plasma" phase is much simpler. (It may well be noticed here, that metals under normal conditions are also simpler than at zero temperatures, at which they are superconductors.)

2. The QCD Vacuum and the Phase Transition into QGP

The most fundamental object of the strong interaction physics is the so called "QCD vacuum", the ground state of this theory. It is filled by a complicated fluctuations of gluonic and quark fields, and during the last decade a "phenomenology of the QCD vacuum" have become rather rich, see review¹⁾. It is based on "three whales": lattice numerical experiments, QCD sum rules and the semiclassical theory of instantons. I comment only on the last one, because here the progress is rather recent and not widely known.

There are two distinct types of waves on the water. There are small-amplitude plane waves, which are described in simple linear approximation, and the "solitons", a solitary wave which is stable due to nonlinearity. The "QED vacuum" can easily be described in terms of "zero point" vibrations of the "field oscillators", the independent small-amplitude waves. Instantons (discovered by Polyakov et al.²⁾ in 1975) are similar to solitons, except for the fact that they are localized not only in space but also in time. It was soon realized that discovery of instantons has opened new perspectives in QCD (see e.g.³⁾), but the so called "dilute gas approximation"

used at that time was found inadequate, so no quantitative predictions have been found. Later phenomenological studies⁴⁾ have lead to the so called "instantonic liquid" model, suggesting that there exist nontrivial "small parameters" in this problem. These ideas are now supported by the lattice studies⁵⁾.

The progress reached during the last few years have now resulted in more or less quantitative theory of this "instantonic liquid". It was due to the variational approach suggested in⁶⁾ and to numerical studies⁷⁾. I am unable to go into details, but try to explain some aspects of this theory important for this talk.

One of the main puzzles of the QCD vacuum is the nonzero ^{average} value of the operator $\bar{\psi}\psi$, the so called "quark condensate". Understanding of its nature is badly needed, say, for the pion physics: we remind that soft pions are nothing else but a long-wave oscillation of the "phase" of this condensate around the value spontaneously selected by the vacuum.

The "instanton liquid" provides an explanation to it. One may understand it by the analogy. Instantons, a localized region with strong color field, are some potential wells for the light quarks. Moreover, there is a definite number of "valence quarks" emitted or absorbed by them. The question is how the "matter" made of such objects is organized: is it a "conductor" or an "insulator". More precisely, do they form some "infinite cluster", or are split into separate "molecules". The former case imply nonzero quark condensate, the latter one means that it is absent. Now this problem is solved: in the "instanton liquid" vacuum the former picture takes place.

Moreover, it is known that if one "heat the vacuum" to some temperature T , the instantons are suppressed and their density is decreasing. It was found⁷⁾, that under

certain conditions transition to "molecular" phase with zero quark condensate value takes place. It is expected that it is strong first-order transition with large jump in all parameters (e.g. in the energy density). It is in many ways similar to the ordinary liquid-gas transition. The latest lattice data agrees with this conclusion⁸⁾.

3. Expansion of QGP and the Phase Transition

The physics of heavy ion collisions at high energies, aiming to produce QGP, is now becoming one of the most rapidly developing fields in high energy physics. Just few years ago there were only several theoretical papers devoted to it, while now it is the topic of many specialized conferences. The progress in experiment is especially striking. In about 5 years the specialists in heavy ion physics have moved, say, from Berkly and Darms tadt to CERN and Brookhaven, have mastered acceleration of nuclei in SPS (200 GeV/nucleon) and AGS (14 GeV/nucleon), created large detectors and in 1986 have taken first data with O^{16} .

Here I can comment only on some points related to this phase transition. The first of them deals with the expansion of the excited matter, created in the collision.

Back in 1953 L.D.Landau have used the hydrodynamics to estimate the effect of the collective maater motion on the transverse momenta of particles produced. Of course, he knew nothing about the phase transition assumed the equation of state of ultrarelativistic gas $\rho = \xi/3$. If so, one finds significant (transverse) collective velocity. However, as noted in⁹⁾, such velocity is not seen, at least in the pp data.

"Scenario no.1" suggested in this work was as follows. Transition of the quark-gluon plasma is assumed to be slow, drops of QGP are "overcooled" into some "bags", be-

ing in mechanical equilibrium. It means that the plasma pressure is balanced by that of the vacuum. If so, there is no pressure gradient and there appears practically no hydrodynamical effects.

"Scenario no.2" was suggested by van Hove¹⁰⁾, it assumes that the QGP can very rapidly turn into the hadronic gas. If so, it happens in the so called "deflagration" shock, in which the system jumps over the mixed phase and instantly transfer the "latent heat" of QGP into collective motion of the pionic gas. Studied by a number of authors it was shown to produce some hydrodynamical effects, which are not very large but observable.

The story became quite intriguing after the report by JACEE cosmic ray experiment¹¹⁾ devoted to high energy nuclear colisions. They have found sharp growth in the average transverse momenta with the "thermolized energy density" (evaluated from the transverse energy per unite rapidity interval). However, in the first data from CERN for O-Pb collisions (e.g.¹²⁾) one does not see strong correlations between mean transverse momenta of secondaries and the "transverse energy" deposited in the particular event.

The models (which experimentals like very much because they are available as the event-generating codes), treating nuclear collisions as a set of independent-nucleon ones (see e.g.¹³⁾) explain it in very simple way: there is no "final state interaction" and respectively no collective effects. Particular versions of such models suggest that all secondaries come from independent "string breaking", proceeding as in ordinary pp collisions. But can one trust this picture, keeping in mind that under these conditions there should be density of strings up to 10-20 per square fermi? Can we imagine, that a pion comes from a cluster of about 500 other had-

rons without any rescattering?

There are some (preliminary) data of the NA38 CERN experiment on the interference correlations of identical pions, which shows that the radius of such cluster at the decay moment is large, about 7 fermis. This is much larger than the oxygen radius, of course, thus direct evidences in favor of "final state interaction" and expansion seem to be there.

The absence of prominent effect in the mean transverse momenta is a quite definite manifestation of "softness" of the equation of state of the excited hadronic matter, the softness being a definite signal of the phase transition in this region. (Let me emphasize, that the conditions for application of the hydrodynamics are now well satisfied: the mean free path of a gluon under such conditions, the energy density equal to few GeV per cubic fermi, is 0.2-0.3 fermi, while the system dimensions are one order of magnitude larger.)

If we come from mean transverse momentum to their distribution, we find noticeable changes while one goes from pp to AA collisions. There appears two components in spectrum. The low p_{\perp} particles have smaller "temperature", about 90 MeV (as the break-up temperature should do for larger systems), while there appear some "tail" with "temperature" about 200 MeV. It either correspond to "evaporated" particles at higher temperatures during the expansion (see e.g. such analysis of the ISR pp data by Zhirov ¹⁴), or the result of "deflagration". The velocity of the deflagration front is low, so estimates show that only fraction of the matter may have time to undergo it. (Note that longitudinal expansion may also cool the matter to the break-up conditions.)

Both mechanism producing such "tail" are very interesting. "Evaporation" should take place during the

"mixed phase" mainly, if the energy density of the plasma and hadronic gas is significantly different. If so, the temperature should mainly be "frozen" at the critical value: with some luck this fact can be detected. The fraction of deflagrated matter should depend on the atomic number in simple way, for it is just geometrical factor. Measurements of heavy particle spectra (say, kaons, anti-protons etc.) may also shed light on whether we have transverse collective flow or not.

Finally some comments on future plans of the experimentalists. This september there be another run at CERN with twice heavier nuclei, S^{32} . It means that people are not afraid to deal with about 1000 particles per event! There are plans to provide lead ion source for CERN SPS. Americal physicists are working on RHIC project in Brookhaven, which is 100 GeV times 100 GeV collider, There is no doubt that QGP will definitely be produced under these conditions. I hope we all together are clever enough to detect its aparence and measure its properties. All is needed is some hard work and some amount of time.

REFERENCES

1. E.V.Shuryak. Phys. Rep. 115C (1984) 152.
2. A.M.Polyakov. Phys. Lett. 59B (1975) 82. A.A.Belavin, A.M.Polyakov, A.A.Schwartz and Yu.S.Tyupkin. Phys. Lett. 59B (1975) 85.
3. Callan C.G., R.Dashen and D.J.Gross. Phys. Rev. D17 (1978) 2717.
4. Shuryak E.V. Nucl. Phys. B203 (1982) 93.
5. M.I.Polikarpov, A.I.Veselov. Instantons and confinement in the SU(2) lattice gauge theory ITEP preprint 41, Moscow 1987.
6. Dyakonov D.I. and V.Yu.Petrov, Nucl. Phys. B245 (1984) 259.

7. Shuryak E.V. Strong correlation of instantons. *Phys. Lett.* in press. Toward the quantitative theory of topological phenomena in gauge theories. 3 preprints Novosibirsk 1987.
8. Karsh F. et al. *Phys. Lett.* 188B (1987) 353.
9. Shuryak E.V. and O.V.Zhirov, *Phys. Lett.* 89B (1980) 253.
10. Van Hove L., *Z. Phys. C* 21 (1983) 93, 27 (1985) 135.
11. Barnett T.H. et al. (JACEE collab.) *Phys. Rev. Lett.* 50 (1983) 2062. Proc. of Int. Conference on Cosmic Ray Physics. v.HE1.4-4 p.164, San Diego 1985.
12. Bamberger A. et al. (NA35 exp) *Phys. Lett.* B184 (1987) 271.
13. Ftacnik J. et al. *Phys. Lett.* 188B (1987) 279.
14. Zhirov D.V. Non-trivial variation of the P slope. Novosibirsk preprint INP 81-31, 1981.

DISCUSSION

G.Soff: You mentioned the dilepton production as a signal of the quark-gluon plasma. There is a recent preprint by Strayer and Boetcher from Oak Ridge who seem to claim that ordinary bremsstrahlung processes create more dileptons than processes which would signal the quark-gluon plasma.

E.V.Shuryak: I do not know this particular preprint, but the general problem is well known. One should find a "window" in dilepton masses between low masses, where bremsstrahlung dominates, and high masses, where the Drell-Yan process dominates. The region 0.5-3 GeV is generally assumed as safe for "plasma signal".

H.Arenhovel: Is there a unique signal for the onset of a quark-gluon plasma which allows the experimentalist to determine the existence of the plasma?

E.V.Shuryak: If some "infinitely large" system be available, then of course "yes" - e.g. the spectrum of e^+e^- does not have resonances like $\rho, \varphi, \psi \dots$. In real collisions the problem is of quantitative comparison and people have to work hard.

E.M.Levin: Is there any difference in production of quark-gluon plasma in hadron-nucleus and nucleus-nucleus collisions?

E.V.Shuryak: The problem is to produce an excited enough system. Obviously, the probability is different in pA and AA collisions, but the corresponding trigger allows to have the same system in both cases.

C.Ciofi degli Atti: If I have understood correctly, you are asking why meson exchange effects are small. The reason is that the experimental data we have considered mostly concern quasi-free kinematics.

I.Rotter: How are the different channels taken into account in the final state interaction for light nuclei?
C.Ciofi degli Atti: For ^2H and ^3He the final state interaction has been taken into account according to Arenhövel and Laget, respectively. For heavier nuclei a simple complex optical potential has been used with no channel coupling. This has to be improved. However, at the largest values of the momentum transfer we have considered, the final state interaction has minor effects.

PHONONS IN SOFT NUCLEI

O.K.Vorov and V.G.Zelevinsky

Institute of Nuclear Physics
 630090, Novosibirsk, U S S R

1. Statement of a problem

Theoretical description of low-lying collective excitations in nuclei without well developed rotational spectra is a longstanding¹⁻⁴ controversial problem. Up to now the convincing microscopic solution of the problem does not exist. In the classical picture³ this motion is interpreted in terms of slow collective vibration of the nuclear field which has the spherical equilibrium shape and acquires time-dependent quadrupole deformation. Self-consistent microscopic consideration of small vibrations in superfluid nuclei can be carried out⁴ in frame of the random phase approximation (RPA). Using it one introduces the new elementary excitation of the boson type, namely the lowest quadrupole phonon. In the microscopic language, it is a boson image of the correlated quasiparticle pair with the angular momentum $\ell = 2$. The phonon wave function is a coherent sum of many ($\Omega \gg 1$) bare two-quasiparticle excitations corresponding to broken Cooper pairs. The enhancement (up to two orders of magnitude) of observed E2-transition probabilities between states apparently of phonon nature is an evident measure of that coherence.

The collectivization degree grows and the phonon frequency drops along with the filling of the valence shell. Here the small parameter $\tau = \frac{\omega}{2E}$ appears where $2E$ stands for the typical energy of the pair breaking. Hence, the collective motion becomes adiabatic and the vibrational amplitude being proportional to $\omega^{-1/2}$ ceases to be small. Therefore the RPA picture is no longer valid and the collective motion should be treated as essentially nonlinear. Taking into account the symmetry principles, one can introduce parameters of the nonlinear interaction of quadrupole phonons in a pure phenomenological way⁵⁻⁷. It allows to evaluate various anharmonic effects. But the parameter number is too big and the phenomenology is not able to offer the dynamic guideline for discriminating the most important terms.

The methodics of boson expansion (BE) of fermion pair operators^{5,8} give the microscopic approach to the regular calculation of anharmonic corrections. Actually, one converts from the two-quasiparticle basis to that of the RPA normal modes which correspond to bosons. Higher orders of BE exceeding the limits of the RPA describe the interaction between the modes as well as their non-boson kinematics. Up to now, various specific algorithms of BE⁸⁻¹², for all their complicacy and tediousness, cannot be considered as quite satisfactory. In particular, it is difficult to take into account properly the coherent response of many noncollective degrees of freedom to slow collective motion. Apart from that, for the noncollective roots of the RPA the convergence of BE is poor.

During the last decade, the interaction boson model (IBM¹³⁻¹⁶) has served as a main tool for the description of low-lying collective states. The rise in the interest to this field is connected just with the great success of the IBM in the phenomenological fit of data. Ho-

wever, the literal identification of s- and d-bosons with images of fermion pairs with angular momenta $\ell = 0$ and $\ell = 2$, respectively, leads to the strict conservation of the boson number in processes of their interaction. This is, in some sense, the "central dogma" of the IBM. Apparently, the convincing theoretical or experimental evidences in favour of such a hypothesis are lacking¹⁷. From the microscopic point of view, such an assumption discards the important parts of the quasiparticle interaction in the particle-hole channel.

The approach developed by the authors¹⁸⁻²⁵ is based on the analysis of the experimental data together with the reliable points of previous theoretical considerations.

2. The semimicroscopic model of nonlinear vibrations

The theory is formulated in terms of quadrupole phonons which are the bosons originated from the RPA normal modes in a nucleus with pair correlations^{3,4}. The collective adiabatic quadrupole mode exists in nuclei with several valence nucleons. Both pairing and strong particle-hole interaction are turned out to be necessary for its emergence. Phonons are interacting via processes of their virtual decay into quasiparticles. Using experimental parameters of collectivity ($\Omega \gg 1$) and adiabaticity ($\tau \ll 1$) connected in typical soft spherical nuclei with the relation $\Omega \tau^3 \sim 1$ one can make simple estimates¹⁹ of anharmonic effects. Such an estimate shows that the amplitude γ for the decay of a phonon into two quasiparticles has the same order of magnitude as the phonon frequency, $\gamma \sim \omega$. Actually, the nucleus is on the threshold of the phase transition where the soft mode under study is almost unstable. Thus, the role of nonlinear effects

becomes decisive. As distinct from macroscopic systems, the transitional region is rather extensive since the adiabatic parameter (large vibrational amplitude) can compensate the small factor ($\Omega^{-1/2}$) which determines the degree of distortion of each simple excitation contributing to the collective mode.

Drawing on the estimate $\psi \sim \omega$ one can score anharmonic effects on a specific scale¹⁹. Skeleton graphs for nonlinear processes are fermion loops L_n with n phonon tails (similar to the diagrams of photon by photon scattering in quantum electrodynamics). For even n , one obtains readily $L_n \sim \omega \tau^{n-4}$, i.e. the dominance of quartic anharmonicity ($n = 4$) which is strong, $L_4/\omega \sim 1$. Odd- n terms are suppressed by the approximate particle-hole symmetry (similar to the Furry theorem) whereas higher order even- n terms contain too many energy denominators. Among the quartic terms, the most important, according to the adiabaticity criterion, are those correcting the potential energy, i.e. containing $(d + d^\dagger)^4$. Here d_μ (d_μ^\dagger) is the annihilation (creation) operator for the quadrupole phonon with the projection μ of the angular momentum. Thus, contrary to the IBM, the phonon number does not conserve.

In conformity with the discrimination of anharmonic terms, we start with the effective phonon hamiltonian of the leading order

$$H_0 = \frac{1}{2} \sum_{\mu} (\pi_{\mu}^{\dagger} \pi_{\mu} + \tilde{\omega}^2 d_{\mu}^{\dagger} d_{\mu}) + \Lambda (\sum_{\mu} d_{\mu}^{\dagger} d_{\mu})^2 \quad (1)$$

where $\tilde{\omega}$ is the phonon frequency in the linear approximation, $d_{\mu} = (2\tilde{\omega})^{-1/2} d_{\mu}^{(+)}$ stands for the collective coordinate and $\pi_{\mu} = -i(\tilde{\omega}/2)^{1/2} d_{\mu}^{(-)}$ for the conjugate momentum, $d_{\mu}^{(\pm)} = d_{\mu} \pm (-1)^{\mu} d_{-\mu}^{\dagger}$ and Λ is the parameter of the quartic anharmonicity. If one is interested

in relative energies of levels, the hamiltonian has only one parameter. In standard Bohr variables, the potential (1) is $\frac{1}{2} \tilde{\omega}^2 \beta^2 + \Lambda \beta^4$. Remarkably enough, this simplified hamiltonian (1) contains already main qualitative features of spectra of soft nuclei. Therefore, it can substitute the crude harmonic approximation ($\Lambda = 0$) as a standard for vibrational and transitional nuclei. In more exact calculations, one can add to the hamiltonian (1) anharmonic corrections of next orders.

3. O(5) symmetry and phonon condensate

The unique feature of the quartic hamiltonian (1) is the O(5)-invariance. It persists²¹ even if quartic terms depending on momenta π_{μ} are included. Thus, microscopic estimates lead to the prediction of the new dynamical symmetry, namely O(5) symmetry, which should characterize spectra of soft nuclei. Independently of the strength of quartic anharmonicity, the five-dimensional momentum (phonon seniority) ν should be a good quantum number. Experimental data support this idea. O(5) classification of levels works well in all soft nuclei being compatible with strong deviations from the pure harmonic approximation.

To get the qualitative understanding, it is instructive to remind the results¹⁸ of the approximate analytic solution for the hamiltonian (1). Labeling the excited states at the fixed value of the seniority ν by the additional quantum number n one can write down the energy spectrum $E_{\nu, n}$ for small n as

$$E_{\nu, n} = \omega_{\nu} \left\{ \frac{3 + (\tilde{\omega}/\omega_{\nu})^2 (\nu + \frac{5}{2})}{4} + 2n \left[1 + \lambda_{\nu} (3n + \nu + \frac{1}{2}) \right] \right\}. \quad (2)$$

Here ω_{ν} is the frequency of the optimal effective linear oscillator in the sector with given ν . It should

be found from the simple equation

$$\omega_v^3 - \tilde{\omega}^2 \omega_v = 4(v + \frac{7}{2})\Lambda. \quad (3)$$

The renormalized coupling constant λ_v in (2) is small independently of the starting anharmonicity Λ ,

$$\lambda_v = \frac{\Lambda}{\omega_v^3} = \frac{1 - (\tilde{\omega}/\omega_v)^2}{4(v + \frac{7}{2})} < \frac{1}{4(v + \frac{7}{2})} \leq \frac{1}{14} \quad (4)$$

In the same approximation one can obtain easily wave functions for states $|v, n\rangle$. In the basis of states with the definite phonon number N these functions are the broad packets which correspond to the strong nonconservation of N . Nevertheless, introducing formally $\tilde{N} = 2n + v$, it is possible to reduce the level classification to that of the harmonic five-dimensional vibrator with new energy intervals (2).

The physical pattern emerging from this approximate solution is²⁶⁾ that of the condensate of pairs of the bare bosons. Due to the compensation of dangerous graphs, this condensate at each value of v is optimal from the energetic point of view. The condensate determines the mean square value of the five-dimensional radii β^2 which depends on v (the analogue of the centrifugal energy). The accuracy of the approximation grows with v increasing. It is quite understandable in the geometric picture similar to the $1/N$ -expansion in the field theory. Important is that the condensate is $O(5)$ invariant, i.e.

γ -unstable. The static deformation of the definite sign (prolate or oblate) could rise due to the cubic (or higher order) corrections violating the symmetry.

4. The model of nonlinear vibrations and the experiment

The simple pattern predicted by the $O(5)$ -symmetric model is revealed in spectra of many nuclides (^{98}Ru , ^{100}Pd , ^{102}Cd , $^{132,140}\text{Xe}$, ^{148}Sm , $^{150,152}\text{Gd}$, ^{154}Dy and so on). In some cases, for example in the yrast band of ^{100}Pd , the predictions are satisfied almost exactly in the asymptotic limit of the pure quartic anharmonicity ($\tilde{\omega} \rightarrow 0$), i.e. without any parameter¹⁹⁾. For remaining cases, it is necessary to add to the boson condensate the "virtual rotation"^{17,19,25} resulting from the coherent nucleon response to the slow vibrating dynamic deformation. It splits the levels (for example, 2_2^+ and 4_1^+) which are degenerate in the $O(5)$ scheme but have different angular momenta. The corresponding contribution to the moment of inertia varies systematically along the shell filling. In average it is close to the rigid body moment of inertia. It shows that the main correlation effects rising the typical rotational energy up to its actual value are accumulated in the quartic anharmonicity. Such systematics turn to be valid even for ground bands in well deformed nuclei.

Finally, incorporation of the weak cubic anharmonicity ($\sim \beta^3 \cos 3\gamma$) leads to the complete three-parameter phenomenological description of spectra of a great number of isotopes. As an illustrative example we show (Fig. 1) the calculated relative energies for the whole set of low-lying states (17 levels) in ^{110}Pd as compared with experimental data. The description quality proves to be typically better than in the phenomenological IBM fits the latter having usually more free parameters.

In several cases, the model of nonlinear vibrations gives the best agreement with data if $\tilde{\omega}^2 < 0$, i.e. for the RPA solution being unstable. The stability is resto-

red by the quartic potential. Then the levels with high seniority localized far away from the origin get into the attraction pocket so that their energy goes down. Such a behaviour manifests itself, in particular, by the abnormal lowering of 0^+ levels in Pt isotopes. This qualitative phenomenon is usually explained in the frame of the IBM by the specific $O(6)$ symmetry of the hamiltonian²⁷. Here it is a special case of the general theory.

To calculate transition probabilities, one must construct, on the same microscopic grounds, the transition operators of a desirable symmetry expressed in terms of phonon variables $d_{\mu}^{(\pm)}$. The diagrammatic structure of the phonon interaction terms implies that each contribution to the phonon hamiltonian generates the corresponding component of the quadrupole operator according to $Q_{\mu} \sim \delta H / \delta d_{\mu}^{(\pm)}$. Therefore in our model the quadrupole tensor should contain, apart from the conventional linear term, corrections due to the anharmonicity

$$Q_{\mu} = d_{\mu}^{(+)} + \alpha (d^{(+)})_{2\mu}^3 + Q'_{\mu} \quad (5)$$

where the second term reflects the quartic anharmonic effects and Q' is generated by the cubic anharmonicity and by the virtual rotation. The last term (5) is responsible for the expectation values of the quadrupole moment and for the crossover transition and slightly changes the allowed (collective) transition probabilities²⁵.

The specific feature of the quartic anharmonicity is the second term in the operator (5). The new parameter α makes it possible to describe consistently the typical experimental pattern, namely attenuation with J of probabilities of main quadrupole transitions $J \rightarrow J-2$ along the yrast line, suppression of the $0_2 \rightarrow 2_1$ transition comparing with the harmonic approximation and pre-

sence of weak E2 transitions with $\Delta N = 3$. Fig. 3 demonstrates the natural explanation of yrast-cascade probabilities for various nuclei obtained for close values of α from zero to -0.4 . Any artificial hypotheses concerning the cut-off of phonon bands due to the depletion of the collective space become redundant. It is interesting that the one-parameter formula (5) with the term Q' omitted gives a reasonable agreement with the transition probabilities along yrast bands in deformed nuclei up to high angular momenta, $J \sim 30$, (see Fig. 4) at the value of α close to that in soft spherical nuclei. Fig. 5 shows the comparison of calculated E2-probabilities with data available for Ru and Pd isotopes. Here additional terms Q' have been taken into account so that the total fit contains three parameters. With the same values of parameters the expectation values of quadrupole moments for 2_1^+ states were also calculated (Fig. 6). In analogous way, one can describe satisfactorily the data on M1 transitions. It is well known that, as a rule, collective models encounter difficulties in the description of magnetic effects in the quadrupole collective motion.

The parameter values giving the best fits agree with the microscopic estimates in the most cases. The quartic anharmonicity indeed turns out to be strong whereas the cubic one is typically weak with the exception of the shell boundaries. The model of nonlinear vibrations with the minimum parameter number works well practically for all spherical nuclei so that we could not find any serious discrepancies with data. A number of the IBM assumptions can be discarded and the logical connection with the traditional picture of the low-lying collective motion can be kept. As distinct from the previous extensive many-phonon calculations⁷, here one does not need usually to diagonalize large matrices. The main effects have

been isolated by means of preliminary microscopic estimates. It furnished an explanation of the qualitative trends as well as knowledge of relative values of parameters.

5. Towards the complete theory

The self-consistent microscopic computation of model parameters is still the most important open problem. The complexity of the problem roots in the large vibrational amplitude of the mean spherical field. Standard methods²⁸ of derivation of a collective adiabatic hamiltonian encounter here serious difficulties. The point is that one needs to consider the frozen nuclear field brought, with the aid of some constraint, to the non-equilibrium quadrupole deformation. This field is used then to construct the travelling quasiparticle basis which is necessary for the calculation of the collective potential energy and the inertial tensor. However, such a deformed field being equivalent to the deformed phonon condensate violates the spherical symmetry ($O(3)$ as well as $O(5)$). Meanwhile, our phenomenology is based, in agreement with data, on $O(3)$ and $O(5)$ symmetries. Therefore one needs the theory with the symmetric condensate.

In this direction it is possible to bridge the gap between our approach and that of the IBM. The main difference is that our condensate is formed by the d-boson pairs coupled to the zero angular momentum without violating the seniority rather than by single d-bosons.

In such a situation, the BE method can serve for tentative estimates only since the expansion of fermion operators are built in this method above the old vacuum state. Most promising are two possibilities: (i) straightforward mapping of exact fermion operator equation of motion onto the boson dynamics and (ii) variational approach generalizing the BCS theory to take into account both

standard Cooper pairs ("s-condensate") and quadrupole phonon pairs ("d-condensate"). Studies in these directions are in progress.

R e f e r e n c e s

1. N.Bohr and F.Kalckar. Dan. Vid. Selsk. Mat.-Fys. Medd. 14, N 10 (1937).
2. A.Bohr. Dan. Vid. Selsk. Mat.-Fys.Medd. 26 N 14 (1952).
3. A.Bohr and B.Mottelson. Nuclear Structure, vol.2. Benjamin, 1975.
4. S.T.Belyaev. Dan. Vid. Selsk. Mat-Fys. Medd. 31 N 11 (1959).
5. S.T.Belyaev and V.G.Zelevinsky. JETP, 42 (1962) 1590.
6. B.E.Stepanov. Yad. Fiz. 18 (1973) 999.
7. G.Gneuss, U.Mosel and W.Greiner. Phys. Lett. 30B (1969) 397; 31B (1970) 209; 32B (1970) 161.
8. S.T.Beliaev and V.G.Zelevinsky. Nucl. Phys. 39 (1962) 582.
9. T.Marumori, M.Yamamura and A.Tokunaga. Progr. Theor. Phys. 31 (1964) 1009.
10. P.Ring and F.Schuck. Phys. Rev. C16 (1977) 801.
11. E.R.Marshalek. Nucl. Phys. A347 (1980) 253.
12. T.Tamura, K.Weeks and T.Kishimoto. Phys. Rev. C20 (1979) 307; Nucl. Phys. A347 (1980) 359.
13. A.Arima and F.Iachello. Ann. Phys. 99 (1976) 253; 111 (1978) 201; 123 (1979) 468.
14. P.O.Lipas. Int. Rev. Nucl. Phys. 2 (1984) 33.
15. R.V.Jolos, I.Kh.Lemberg and V.M.Mikhailov. Elem. Part. Nucl. Phys. 16 (1985) 280.
16. A.E.L.Dieperink and G.Wenes. Ann. Rev. Nucl. Part. Sci. 35 (1985) 77.
17. V.G.Zelevinsky. Sov. Phys. Izvestia, ser. fiz. 48 (1984) 79.
18. O.K.Vorov and V.G.Zelevinsky. Yad. Fiz. 37 (1983)1392.

19. O.K.Vorov and V.G.Zelevinsky. Nucl. Phys. A439 (1985) 207.
20. V.G.Zelevinsky. In: Nuclear structure. Dubna, 1985, p.173.
21. O.K.Vorov and V.G.Zelevinsky. Preprints INP 84-137, 85-120, Novosibirsk.
22. V.G.Zelevinsky. In: Nuclear Structure, Reactions and Symmetries. Dubrovnik, 1986.
23. O.K.Vorov and V.G.Zelevinsky. Sov. Phys. Izvestia, ser. fiz. 51 (1987), 66.
24. O.K.Vorov. Preprints INP 86-86, 86-150, Novosibirsk.
25. O.K.Vorov and V.G.Zelevinsky. Proc. of XXI LINP winter school. Leningrad, 1986, p.195.
26. V.G.Zelevinsky. JETP, 46 (1964) 1853.
27. R.F.Casten. Nucl. Phys. A347 (1980) 173.
28. S.T.Belyaev. Nucl. Phys. 64 (1965) 17.

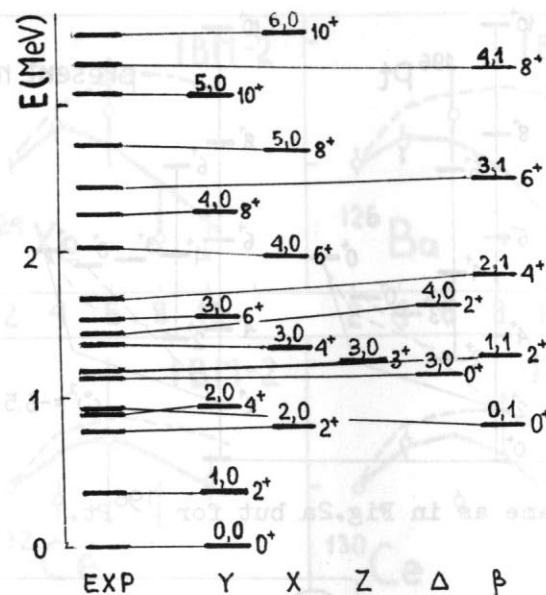


Fig. 1. Energy levels in ^{110}Pd : experiment and calculation in the present model. Values of v , n , and J^P are marked for each level.

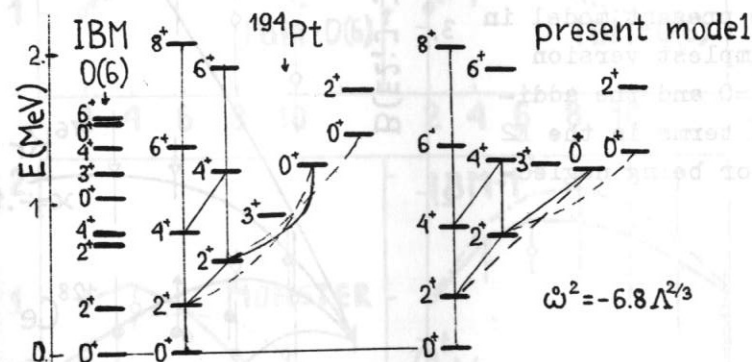


Fig. 2a. The same as in Fig.1 but for ^{194}Pt . IBM-results are also presented (on the left). Enhanced $E2$ transitions and reduced ones are marked by solid lines and dashed ones respectively.

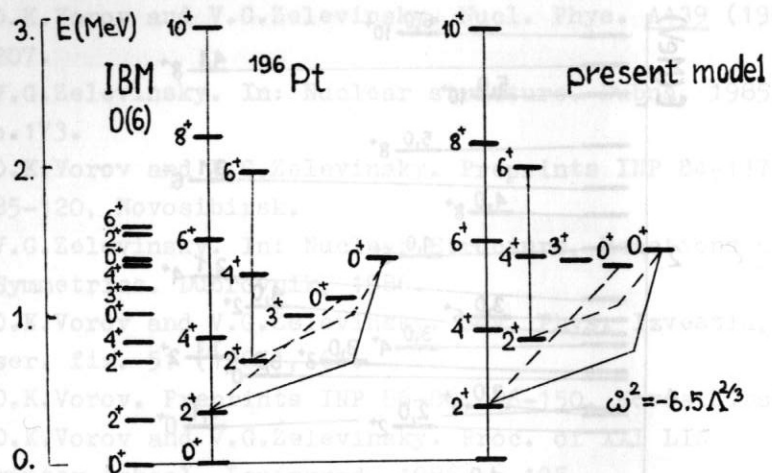


Fig. 2b. The same as in Fig.2a but for ¹⁹⁶Pt.

Fig. 3a. $B(E2)$ values for the yrast-cascades in several isotopes of Se, Kr, and Ce compared with those calculated in the present model in its simplest version (for $\omega=0$ and the additional terms in the $E2$ operator being neglected).

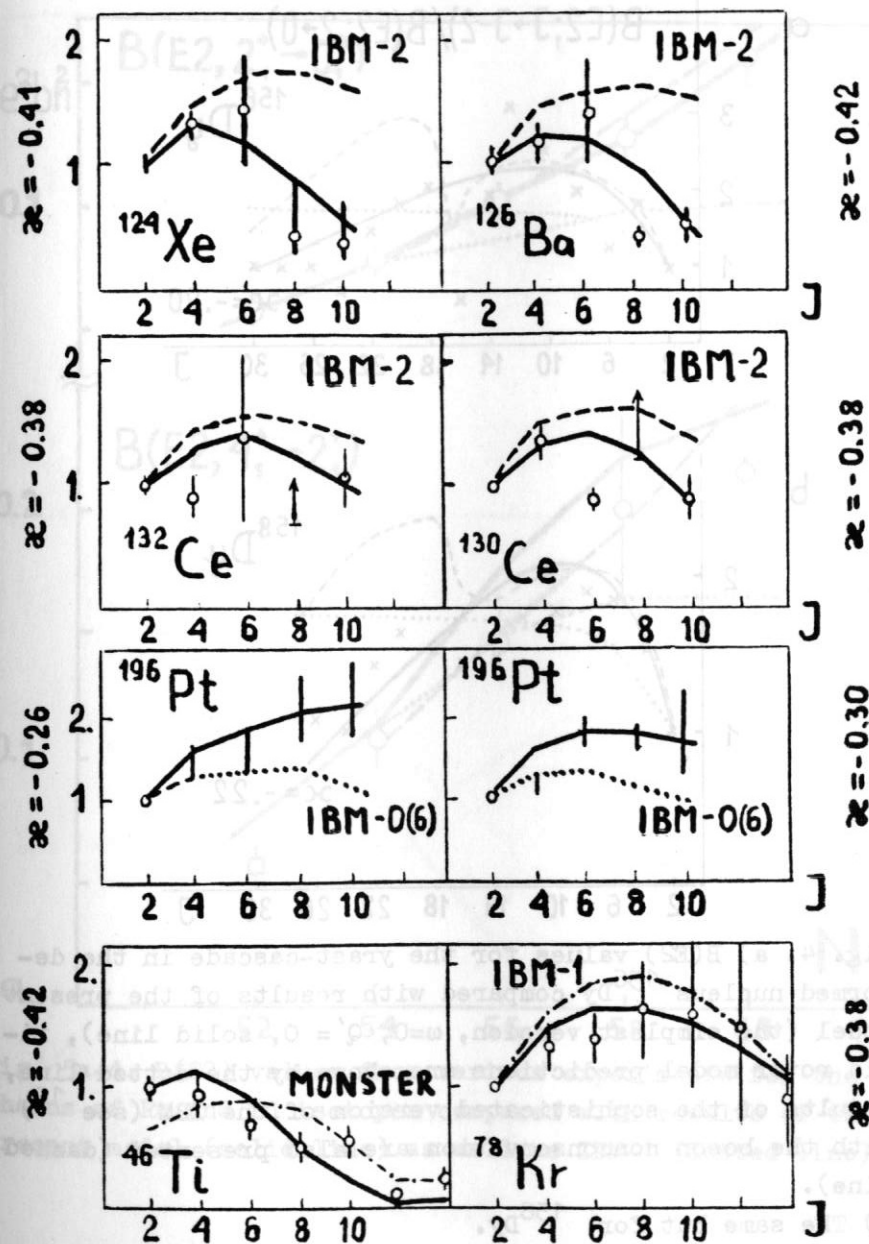
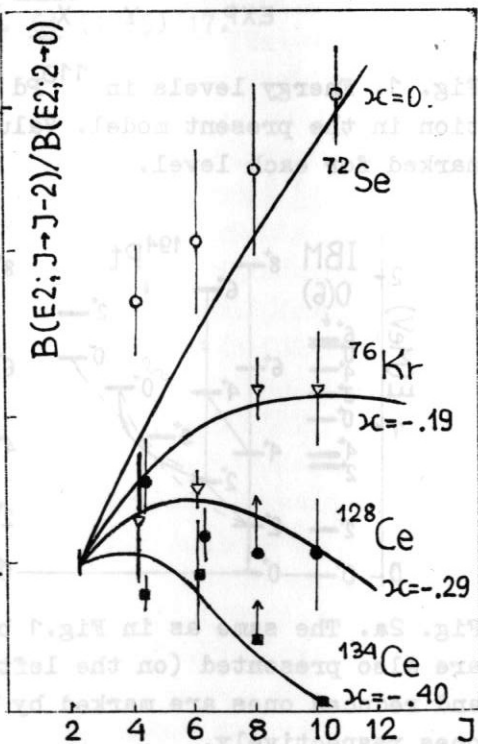


Fig. 3b. The same as in Fig.3a (solid lines - for the present model) in comparison with other models.

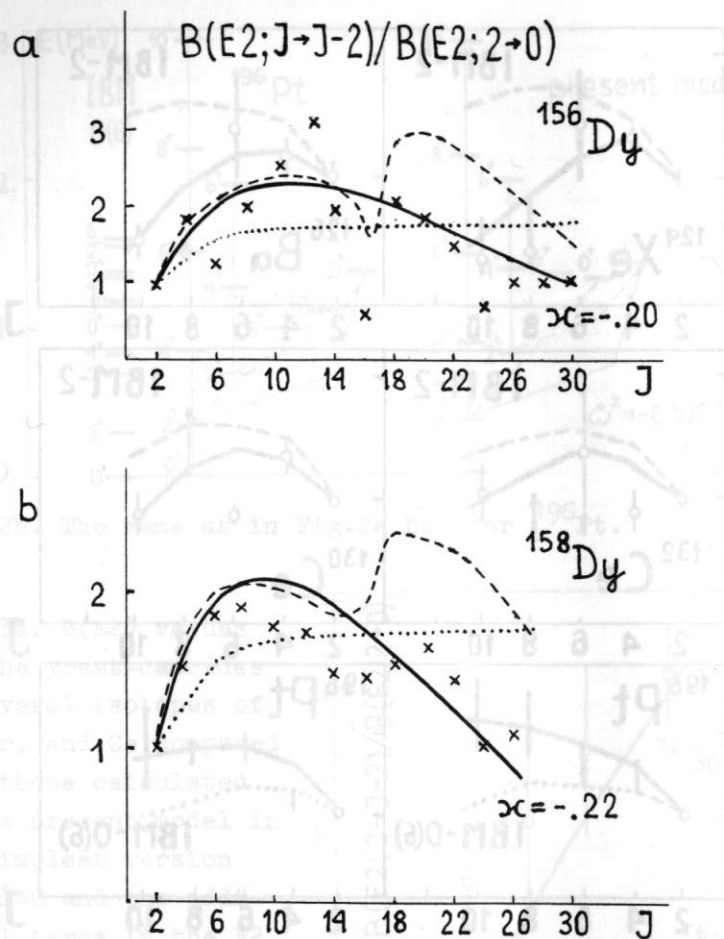


Fig. 4. a) $B(E2)$ values for the yrast-cascade in the deformed nucleus ^{156}Dy compared with results of the present model (the simplest version, $\omega=0$, $Q'=0$, solid line), rigid rotor model predictions are shown by the dotted line, results of the sophisticated version of the IBM (see ¹⁵) with the boson nonconservation are also presented (dashed line).

b) The same but for ^{158}Dy .

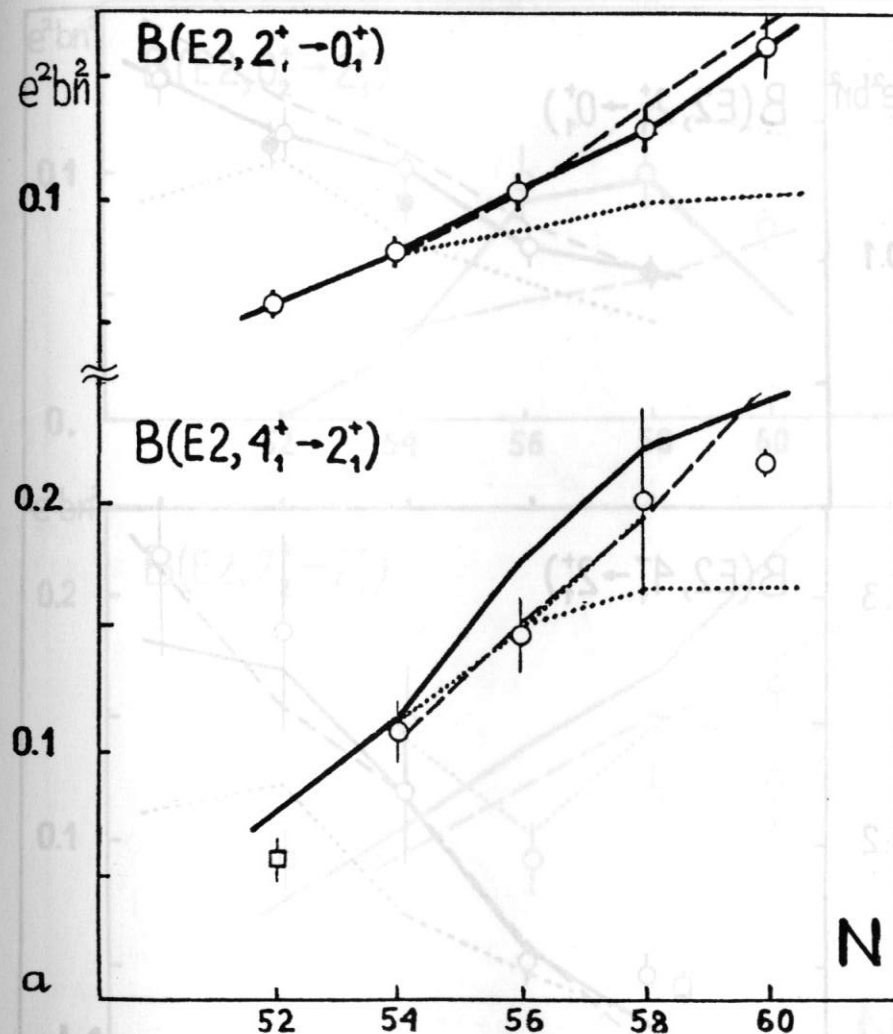


Fig. 5a-d. $B(E2)$ values from various experiments for the chains of Ru and Pd isotopes compared with results of the present model (solid line) as well as IBM-1 (dotted line).

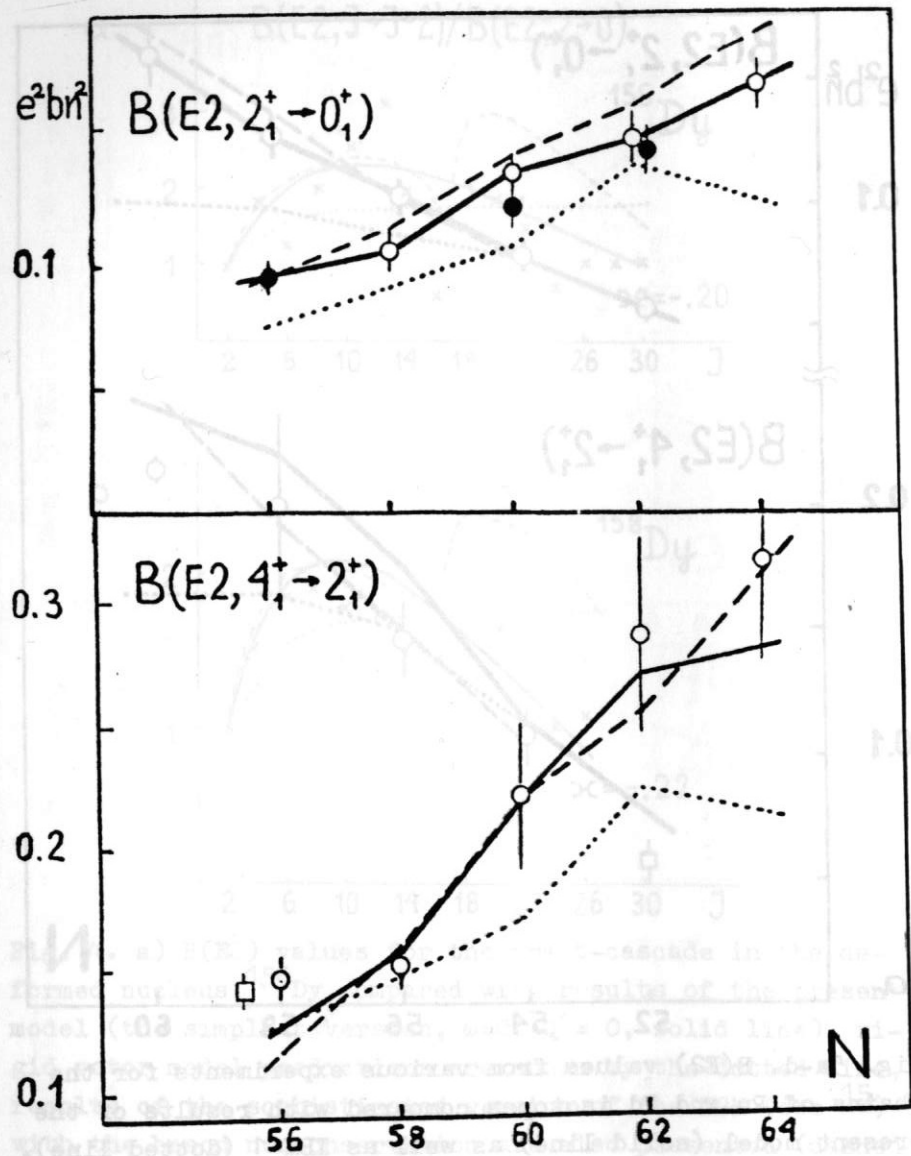


Fig. 5b.

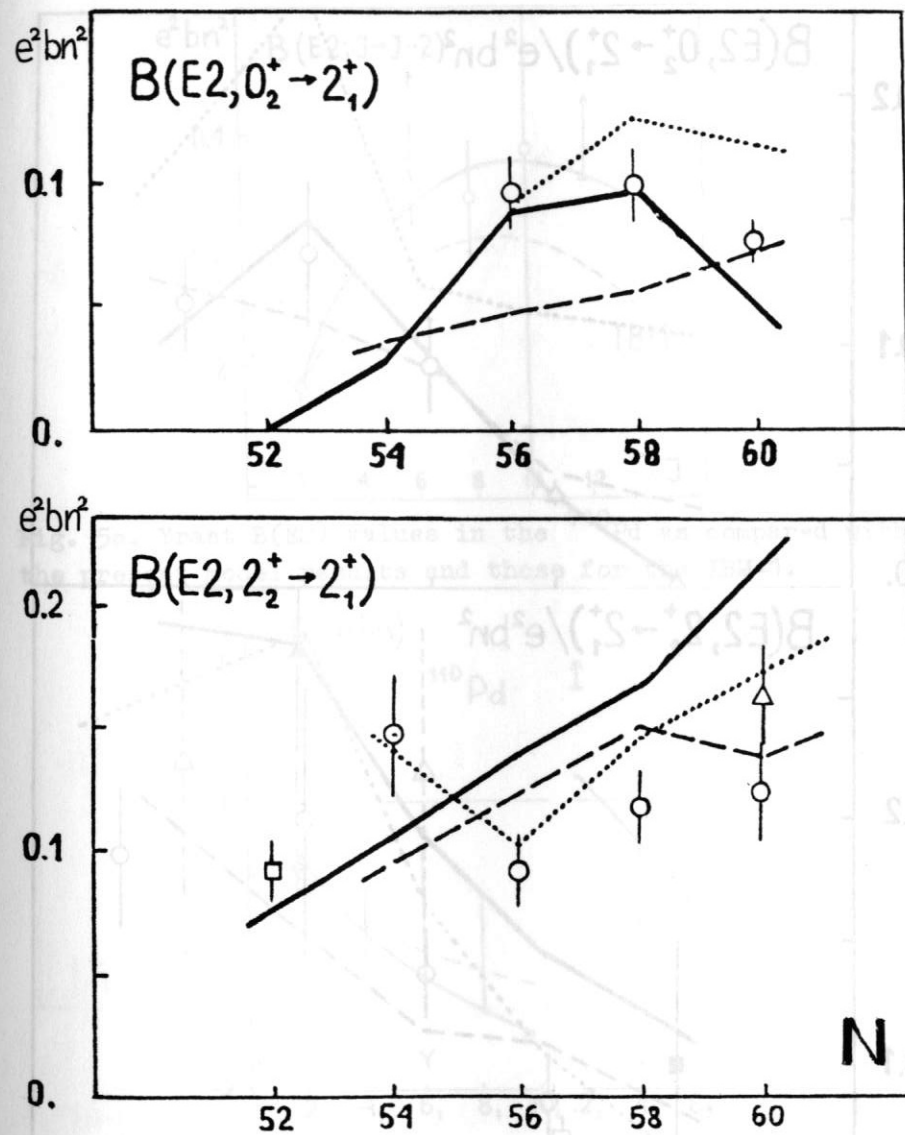


Fig. 5c.

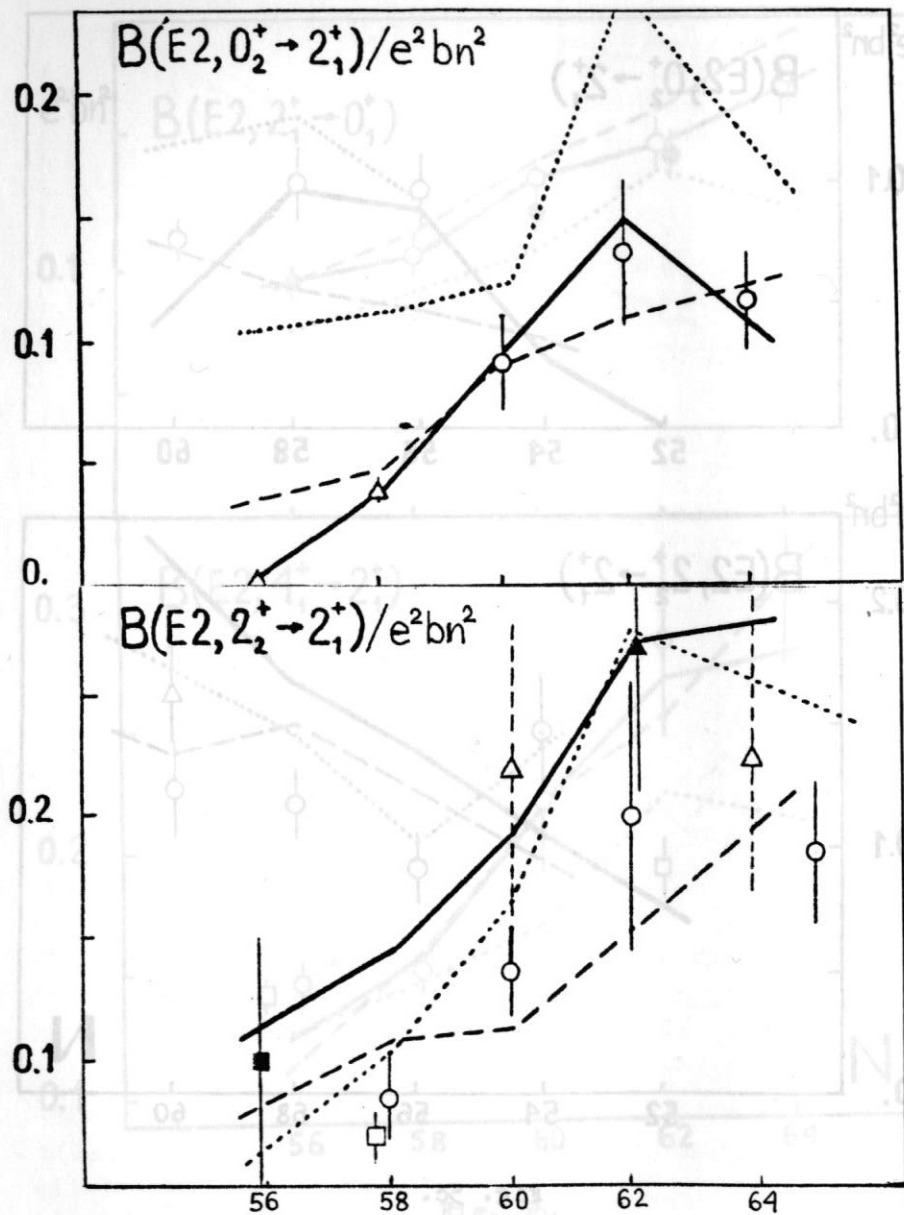
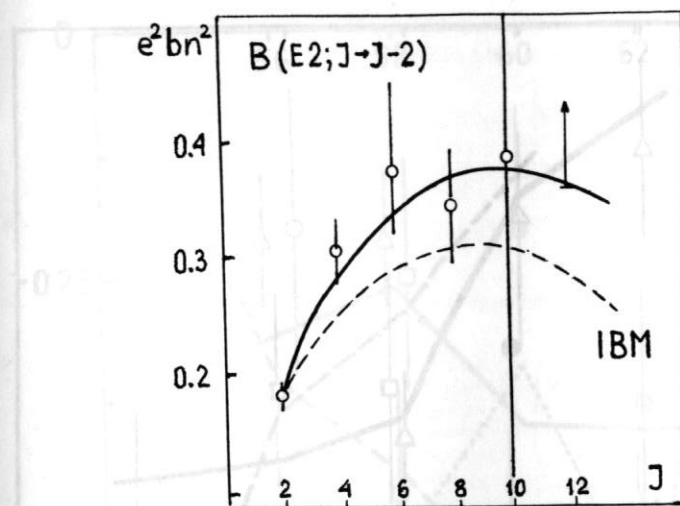
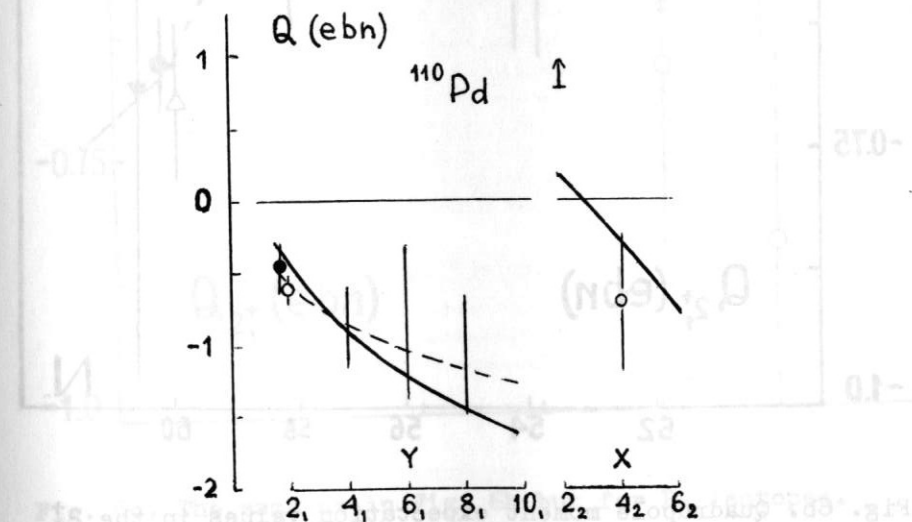


Fig. 5d.

Fig. 5e. Yrast $B(E2)$ values in the ^{110}Pd as compared with the present model results and those for the IBM-1.Fig. 6a. Quadrupole moment expectation values for the yrast band (left part) and for the X-band in ^{110}Pd compared with results of the present model (solid line) and those of the IBM-1 (dashed line).

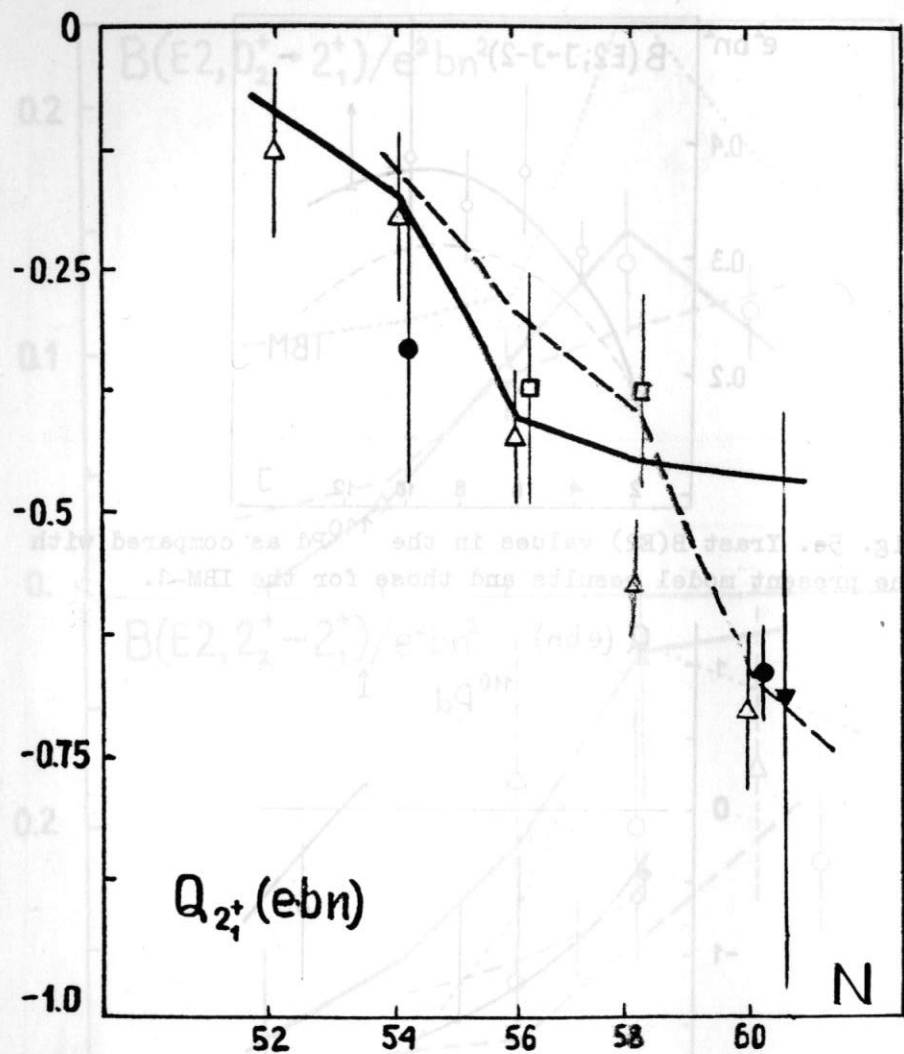


Fig. 6b. Quadrupole moment expectation values in the 2^+_{1} states of Ru isotopes - various experimental data and results of the present model (solid line), IBM-2 (dashed line), and the IBM-1 (dotted line).

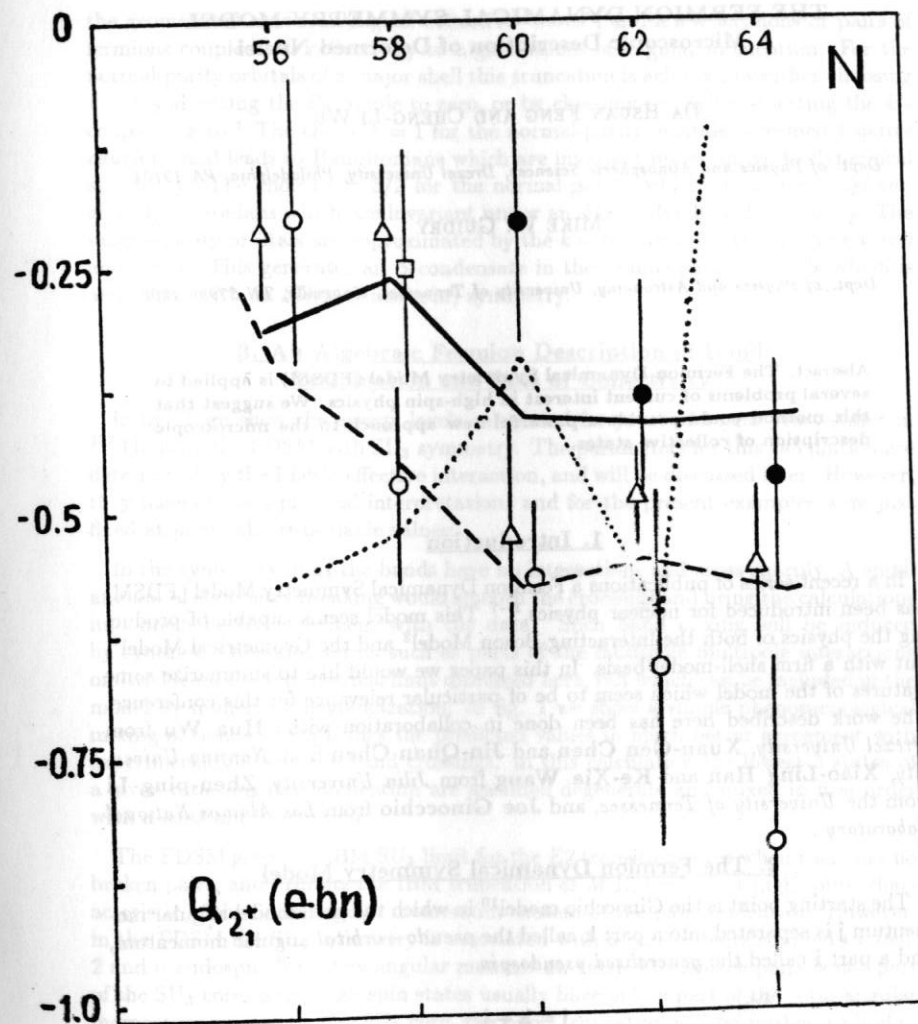


Fig. 6c. The same as in Fig. 6b but for Pd isotopes.

- 16) M. Chemtob and B. Desplanques, Nucl. Phys. **B78** (1974) 139.
 17) T. Goldman and D. Preston, Nucl. Phys. **B217** (1983) 61.

PARITY NON-CONSERVATION IN NEUTRON
 REACTIONS WITH HEAVY NUCLEI

V.V.Flambaum and O.P.Sushkov

Institute of Nuclear Physics

630090, Novosibirsk, U S S R

A b s t r a c t

The general theory of parity non-conservation (PNC) in compound nuclei is considered. We suggest the method of revealing of dominant PNC-mechanism. The PNC-effects in neutron optics and in fission of nuclei are considered in detail.

Introduction

The parity non-conservation (PNC) in nuclear forces was discovered in the reaction $^{113}\text{Cd}(n,\gamma)[1]$. Then the PNC effects were observed in various nuclear reactions. The review of early works one can find in Ref.[2]. Very important step had been done in 1977. We mean the discovery of PNC in fission of nuclei by polarized neutrons [3]. In contrast with the PNC effects which had been observed before, the PNC in fission is manifested in the motion of a nearly macroscopic object: a fragment consisting of about 100 nucleons. The review of early works on this subject is presented in Ref.[4]. The modern review one can find in book [5].

The neutron optics is the other very important way of PNC investigation. The PNC effects in neutron optics were

first observed in 1980. It was the rotation of the cold neutron spin around the direction of the motion in ^{117}Sn [6] and difference in the total cross section for the left and right-polarized thermal neutrons [6,7]. In 1981 the PNC difference of neutron capture cross section near a p-wave compound resonance was observed [8]. The review of works in neutron optics one can find in paper [9] and in book [5].

In present paper the general problems of PNC in neutron reactions are considered. As an example we discuss the PNC in neutron optics and PNC in nuclear fission.

The PNC weak interaction of a nucleon in a nucleus can be described by the effective Hamiltonian

$$H_w \sim G \frac{\vec{\sigma}}{2m} \{ \vec{p}, \rho \} \quad (1)$$

where $G = 10^{-5}/m^2$ is the Fermi constant; $\vec{\sigma}$, \vec{p} , m are the spin, momentum and mass of a nucleon; and ρ is the nuclear density. A magnitude of the mixing of single-particle levels of opposite parity is the ratio H_w/ω , where $\omega \sim p^2/2m$ is the typical energy of the nucleon. In a nucleus we have $p \sim m_\pi$ and $\rho \sim m_\pi^3$, so that

$$F \sim H_w/\omega \sim G m_\pi^2 = 2 \cdot 10^{-7} \quad (2)$$

Of course this estimate is very crude, but more realistic calculation shows that eventually the magnitude $F \sim G m_\pi^2 = 2 \cdot 10^{-7}$ is reasonable.

Usually the magnitude of PNC effects in compound nuclei is of the order of $\sim 10^{-4}$. The enhancement in comparison with F is due to the high level density [10-12]. Following Ref. [12] we will refer to this effect as "dynamic enhancement".

I. The matrix elements of single-particle operators

Let us represent the wave function of a compound state as an expansion in products of single-quasiparticle wave functions.

$$\psi = \sum C_\alpha \varphi_\alpha \quad (3)$$

where $\varphi_\alpha = a_1^+ \dots b_1^+ \dots |0\rangle$ are the states which contain a fixed number of particles and holes (a^+ , b^+ are the creation operators for particles and holes).

The number of the "principal" components in ψ (the components which give the main contribution to normalization) is equal to (see Refs. [13-16])

$$N \sim \frac{\pi}{2} \frac{\Gamma_{\text{spe}}}{D} \sim 10^4 - 10^6 \quad (4)$$

Here, D is the average distance between the compound levels, and $\Gamma_{\text{spe}} \sim \text{MeV}$ is the spread width of the state φ_α . Due to normalization for principal components $|C_\alpha| \sim 1/\sqrt{N}$. The components φ_α distant from the energy of compound state ($|E_\varphi - E_\psi| > \Gamma_{\text{spe}}/2$), appear in ψ with a smaller weight [13].

$$|C_\alpha| \sim \frac{\Gamma_{\text{spe}}/2}{E_\psi - E_\varphi} \frac{1}{\sqrt{N}} \quad (5)$$

Let us estimate now the matrix element of a one-body operator \hat{M} between the compound states [10, 17, 15, 16].

$$\begin{aligned} M_{fi} &= \langle f | \hat{M} | i \rangle = \langle \sum_\alpha a_\alpha \varphi_\alpha | \hat{M} | \sum_\beta b_\beta \varphi_\beta \rangle = \\ &= \sum_{\alpha\beta} a_\alpha^* b_\beta \langle \varphi_\alpha | \hat{M} | \varphi_\beta \rangle \end{aligned} \quad (6)$$

With a fixed α , the matrix element $\langle \varphi_\alpha | \hat{M} | \varphi_\beta \rangle$ is non-zero at a few values of β when φ_β differs from φ_α

by the state of one particle only. It is natural to suppose that the signs of particular terms in the sum (6) are random. If we assume that $N_f \lesssim N_i$ then we have the incoherent sum of $\sim N_f$ terms, each of the order of $M^{(1)}/\sqrt{N_i N_f}$. Here $M^{(1)}$ is the typical single-particle matrix element. As a result of summation we have

$$|M_{fi}| \sim \frac{M^{(1)}}{\sqrt{N_i}} \quad (7)$$

In the above estimate, we suppose that the matrix element between the principal components of the states $|i\rangle, |f\rangle$ is not vanished. However, by virtue of the selection rules this matrix element can prove to be zero. Such a situation occurs for the matrix element of weak interaction between the close compound states^[17]. The operator of weak interaction H_W has non-zero matrix element only between the single-particle states from different shells. Therefore acting on the principal component of the compound state $|i\rangle$, H_W transfers it to the small component of the compound state $|f\rangle$. Thus, due to eq. (5) the matrix element is suppressed by a factor Γ_{spr}/ω ($\omega \sim 8$ MeV is the splitting between the shells)

$$\langle f | H_W | i \rangle \sim \frac{\Gamma_{spr}}{\omega} H_W^{(1)} / \sqrt{N_i} \quad (8)$$

The mixing of the nearest compound states ($\Delta E \sim D$) is given in magnitude by

$$\alpha \sim \frac{\langle f | H_W | i \rangle}{D} \sim \frac{H_W^{(1)}}{\omega} \sqrt{N} \sim 10^{-4} \quad (9)$$

The ratio $H_W^{(1)}/\omega$ is a typical magnitude of mixing of single-particle levels (see eq. (2)). We see that mixing of compound levels is enhanced by \sqrt{N} times. It is the "dynamical enhancement" of a weak interaction in the

nucleus [10, 11, 12, 15, 16].

2. Classification of amplitudes in powers of $1/\sqrt{N}$

In the preceding section estimates of matrix elements have been obtained for the wave functions of a discrete spectrum. To apply these estimates for transitions to a continuous spectrum, let us normalize the neutron wave function for $E > 0$ in the following way: $\int_{E>R} \psi^2(r) d^3r = 1$, where R is the size of the nucleus. Besides the matrix elements, the expressions for the reaction amplitudes also include the energy denominators $E - E_c + i/2 \Gamma_c$ where E_c, Γ_c are the energy and width of the compound state. These denominators are smaller by a factor of N than the typical single-particle energy scale $\delta E \sim \Gamma_{spr} \sim \omega \sim \text{MeV}$.

Now we can formulate the rules for the classification of amplitudes in powers of the small parameter $1/\sqrt{N} \sim 10^{-2} - 10^{-3}$.

(i) Each vertex of an interaction (neutron capture, electromagnetic, weak, etc.) contains the factor $1/\sqrt{N_{max}}$, where $N_{max} = \max(N_c, N_{c'})$; $N_c, N_{c'}$ are the numbers of the principal components of the nuclear wave functions which enter into the vertex. In the ground state $N \sim 1$ and in the excited one $N \sim \text{MeV}/D$.

(ii) Every Green function of a compound state $|c\rangle$ (at $|E - E_c + i/2 \Gamma_c| \lesssim D$) gives the factor N_c and the resonance energy dependence $D/(E - E_c + i/2 \Gamma_c)$.

It is worth emphasizing that the rules (i) and (ii) yield a mean-square estimate of the amplitude. In principle, fluctuations can occur, which are capable of changing the amplitude relation in each particular case. But because of the large value of parameter \sqrt{N} , the probability of the fluctuations which violates the \sqrt{N} hierarchy

of amplitudes is very small.

Let us consider, for example, an elastic scattering of a slow neutron ($\rho R \ll 1$) on a nucleus in the case when only the channels (n, n) and (n, γ) are open. The amplitude of s-wave scattering is as follows:

$$f = f_0 - \frac{1}{2\rho} \sum_c \frac{g \Gamma_c^{(n)}(E)}{E - E_c + i\frac{1}{2}\Gamma_c} \quad (10)$$

Here $f_0 = -a$, a is the scattering length, $\rho = \sqrt{2m_n E}$, and g is the factor which appears after averaging over the spin projections of the initial nucleus.

If one is interested only in the powers of parameter \sqrt{N} , it is simple to write an estimate of the resonance part f_r plotted in fig. 1. The diagram contains the neutron-capture vertex ($1/\sqrt{N}$), the neutron-emission vertex ($1/\sqrt{N}$), and the Green function of the compound state $(ND/(E - E_c + i\frac{1}{2}\Gamma_c))$, i.e.

$$f_r \sim \frac{D}{E - E_c + i\frac{1}{2}\Gamma_c} \quad (11)$$

Thus, in elastic scattering (without parity violation) the resonance contribution has zero order in powers of \sqrt{N} similar to the potential contribution. It follows from the experimental data on the neutron strength function (see e.g. ref. [13]) that far from the compound resonances, i.e. at $|E - E_c| \sim D/2$

$$\frac{f_r}{f_0} \sim \frac{1}{\rho a} \frac{\Gamma^{(n)}}{D} \sim 0.05 - 0.5 \quad (12)$$

This ratio is determined by the other parameters (besides \sqrt{N}) involved in the consideration of elastic scattering. For example, according to the model considered in ref. [13],

$$\frac{f_r}{f_0} \sim \frac{g \Gamma_{spr}}{\pi M R a [(E - E_a)^2 + \Gamma_{spr}^2/4]} \quad (13)$$

Here R is the nucleus radius, and E_a is the position of the nearest single-particle s-level. It is seen that the other dimensionless parameters are not as large as \sqrt{N} .

Let us now discuss the of parity non-conserving forward elastic scattering amplitude f_{PNC} . The dominant contribution to f_{PNC} comes from the diagrams connected with the mixing by a weak interaction of the levels of the compound nucleus with opposite parity (fig. 2). They contain three vertices $(1/\sqrt{N})^3$ and two Green functions (N^2), i.e.

$$f_{PNC}^{(2)} \sim \sqrt{N} \frac{D}{E - E_s + i\Gamma_s/2} \frac{D}{E - E_p + i\Gamma_p/2} \quad (14)$$

Neutron scattering on the P-odd potential of the nucleus (fig. 3) and on the P-odd potential accompanied by a virtual capture into the resonance (figs. 4 and 5) also gives contributions to f_{PNC} . The diagram in fig. 3 has no \sqrt{N} , because it is not connected with the compound states. The diagrams in figs. 4 and 5 have zero order in \sqrt{N} , as well. Thus, the contribution of diagram 2 is enhanced by a factor of \sqrt{N} as compared with that of diagrams 3, 4 and 5. It is the dynamical enhancement of the weak interaction in heavy nuclei that has been mentioned above. The contribution of the diagrams presented in fig. 3 has been analysed, for example, in refs. [19-22]. As to the diagram 2 it has been considered in ref. [23] (see also refs. [24, 25, 16]). The contributions 4 and 5 has been considered in refs. [26, 27]. Detailed numerical analysis of diagrams is presented in ref. [28]. In agreement with the $1/\sqrt{N}$ -estimation this analysis shows that $f_{PNC}^{(4,5)}$ is small in comparison with $f_{PNC}^{(2)}$.

3. Parity non-conservation in neutron optics

We discuss the reactions with slow neutrons ($pR \ll 1$), therefore we take into account only s and p-wave capture. The wave function of an initial neutron is of the form

$$e^{i\vec{p}\vec{r}} \chi_\alpha = 4\pi \sum_{lm} i^l j_l(pR) Y_{lm}^*(\vec{n}_p) Y_{lm}(\vec{n}) \chi_\alpha \approx \quad (15)$$

$$\approx 4\pi \left\{ Y_{00}(\vec{n}_p) |\ell=0, j=1/2, \alpha\rangle + \frac{i p R}{3} \sum_{mjz} Y_{1m}^*(\vec{n}_p) C_{1m \frac{1}{2} \alpha}^{jjz} |\ell=1, j, jz\rangle + \dots \right\}$$

Here χ_α is the spin function with the spin projection α ; $\vec{n}_p = \vec{p}/p$, $\vec{n} = \vec{r}/r$; $j_l(pR)$ is the spherical Bessel function. Total angular momentum of the neutron is $\vec{j} = \vec{\ell} + \vec{s}$. $C_{lm \frac{1}{2} \alpha}^{jjz}$ is the Clebsch-Gordan coefficient. Let us consider the capture of the neutron into the compound resonance with the angular momentum \vec{j} . If \vec{I} is the angular momentum of the initial nucleus then $\vec{J} = \vec{I} + \vec{j}$ and we can write down the explicit formulae for the amplitudes. The amplitude of the capture into the s-resonance is equal to

$$C_{II_z \frac{1}{2} \alpha}^{JJ_z} T_s(E) \quad (16)$$

The scalar amplitude T_s is normalized on the neutron width of s-resonance: $|T_s|^2 = \Gamma_n^{(s)}(E) \sim E^{1/2}$. The amplitude of the capture into the p-resonance is equal to

$$\sum_{jj_z m} C_{II_z jj_z}^{JJ_z} C_{1m \frac{1}{2} \alpha}^{jjz} \sqrt{4\pi} Y_{1m}^*(\vec{n}_p) i T_{pj}(E) \quad (17)$$

The scalar amplitudes T_{pj} are normalized in such a way: $|T_{p_{1/2}}|^2 = \Gamma_n^{(p_{1/2})} \sim E^{3/2}$, $|T_{p_{3/2}}|^2 = \Gamma_n^{(p_{3/2})} \sim E^{3/2}$, $\Gamma_n^{(p_{1/2})} + \Gamma_n^{(p_{3/2})} = \Gamma_n^{(p)}$. Here $\Gamma_n^{(p)}$ is the neutron width of p-resonance.

Using the expressions (16) and (17) we can calculate any amplitude. For example, the forward elastic scatter-

ing amplitude near the p-resonance is equal to

$$f_p(0) = -\frac{1}{2p} \sum_{jj_z m} C_{II_z jj_z}^{JJ_z} C_{1m \frac{1}{2} \alpha}^{jjz} \sqrt{4\pi} Y_{1m}^*(\vec{n}_p) T_{pj} \times \quad (18)$$

$$\times \frac{1}{E - E_p + i\Gamma_p/2} C_{II_z jj_z}^{JJ_z} C_{1m' \frac{1}{2} \alpha}^{j'j'z} \sqrt{4\pi} Y_{1m'}(\vec{n}_p) T_{pj'}$$

The factor $-1/2p$ is introduced for normalization. After summation over J_z and averaging over I_z we obtain the usual Breit-Wigner formula with $g = (2J+1)/(2(2I+1))$.

$$f_p(0) = -\frac{1}{2p} \frac{g \Gamma_n^{(p)}(E)}{E - E_p + i\Gamma_p/2} \quad (19)$$

It was shown in preceding section that the main contribution to the PNC-amplitude arises from diagrams presented at fig. 2. Now we can write down the explicit formula for forward scattering PNC-amplitude

$$f_{PNC}(0) = -\frac{1}{p} C_{II_z \frac{1}{2} \alpha}^{JJ_z} T_s \frac{1}{E - E_s + i\Gamma_s/2} \langle S|H_w|p\rangle \frac{1}{E - E_p + i\Gamma_p/2} \times \quad (20)$$

$$\times \sum_{jj_z m} C_{II_z jj_z}^{JJ_z} C_{1m \frac{1}{2} \alpha}^{jjz} \sqrt{4\pi} Y_{1m}(\vec{n}_p) (-i T_{pj}^*)$$

Here $\langle S|H_w|p\rangle$ is the matrix element of weak interaction between two compound-states. This matrix element is purely imaginary. After summation over J_z and averaging over I_z in eq.(20) we obtain

$$f_{PNC}(0) = \pm \frac{g}{p} \sum_{s,p\text{-resonances}} \frac{\sqrt{\Gamma_n^{(s)}(E)} (i \langle S|H_w|p\rangle) \sqrt{\Gamma_n^{(p_{1/2})}(E)}}{(E - E_s + i\Gamma_s/2) (E - E_p + i\Gamma_p/2)} \quad (21)$$

The sign \pm corresponds to the helicity of a neutron. The forward scattering amplitude near p-wave resonance is the sum of (19) and (21)

$$f(0) = -\frac{1}{2\rho} \frac{g \Gamma_n^{(p)}(E)}{E - E_p + i\Gamma_p/2} (1 \pm P(E))$$

$$P(E) = 2 \sum_s \frac{i \langle S | H_W | P \rangle}{E - E_s + i\Gamma_s/2} \frac{\sqrt{\Gamma_n^{(s)}(E) \Gamma_n^{(p)}(E)}}{\Gamma_n^{(p)}(E)} \sim 10^{-2} - 10^{-3} \quad (22)$$

We take into account the estimation (19) for the mixing $i \langle S | H_W | P \rangle / (E_p - E_s) \sim 10^{-4}$. For the resonances with $E_p = 1 - 10$ eV the kinematic enhancement factor is equal to $\sim \sqrt{\Gamma_n^{(s)}(E_p) / \Gamma_n^{(p)}(E_p)} \sim 1/\rho R \sim 10^2 - 10^3$. Besides the resonant part of amplitude there is the non-resonant part which is due to the potential scattering and the tails of s-resonances. We will discuss it below.

Near the s-resonance instead of kinematic enhancement $\sim 1/\rho R$ the kinematic suppression $\sim \rho R$ arises. Therefore the effect is small.

Let us consider now the PNC physical effects. Due to the optical theorem the forward scattering amplitude is connected with the total cross section $\sigma_{tot} = 4\pi/\rho \operatorname{Im} f(0)$. Using the eq.(22) we can find the difference in cross sections for the neutrons with positive and negative helicities.

$$\Delta\sigma = \sigma_+ - \sigma_- = \sigma_2 2P(E)$$

$$\sigma_2 = \frac{\pi}{\rho^2} \frac{g \Gamma_n^{(p)}(E) \Gamma_p}{(E - E_p)^2 + \Gamma_p^2/4} \quad (23)$$

It is well known that for low-lying resonances the total width practically coincides with the γ -width. Therefore from eq.(23) we can conclude that $\Delta\sigma_{tot} = \Delta\sigma_\gamma$. This important relation was checked in experiments with thermal neutron [7, 29]. According to eq.(23) the PNC difference $\Delta\sigma$ has Breit-Wigner form. The first observation of this fact have been done in work [8] on p-wave re-

sonance 1.3 eV in ^{117}Sn .

In experiment one usually measures not directly $\Delta\sigma$, but relative difference between the transmission probabilities for right- and left-polarized neutrons $\mathcal{E} = -1/2 \Delta\sigma N \ell$. Here N is the density of target atoms, ℓ is the length of the target. It is clear that ℓ cannot be much larger than the mean free path $\ell_0 = 1/N\sigma$. If resonance dominates in total cross section $\sigma = \sigma_2$ then $\mathcal{E}(\ell = \ell_0) = -P(E)$. However usually there is the non-resonant background and therefore \mathcal{E} is a few times smaller than P . The analysis of experimental data is presented in review [9] (see also ref. [5]). We present at fig. 6 as an example the experimental plot of \mathcal{E} for 0.75 eV resonance in ^{139}La from ref. [30]. The corresponding value $P(E_p) = (7.3 \pm 0.5) \cdot 10^{-2}$ [30] is in agreement with estimation (24).

The other effect of PNC in neutron optics is the rotation of the neutron spin around its momentum direction [19]. The angle of rotation is connected with the refractive index n_\pm and forward scattering amplitude

$$\varphi = \rho \ell \operatorname{Re}(n_+ - n_-)$$

$$n_\pm = 1 + \frac{2\pi N}{\rho^2} f_\pm \quad (24)$$

Using eq.(22) we find

$$\varphi = -\frac{2\pi N \ell g \Gamma_n^{(p)}(E) P(E)}{\rho^2} \frac{E - E_p}{(E - E_p)^2 + \Gamma_p^2/4} \quad (25)$$

The spin rotation was observed only for the cold neutrons. The first observation have been done for ^{117}Sn [6]. The references to the experimental works and comparison with the data on cross section difference one can find in review [9] and book [5].

4. Parity nonconservation in nuclear fission induced by neutron

If The energy is not too high, the fission of a nucleus goes through the following steps: 1) the capture of a neutron and the formation of a hot compound nucleus; 2) the cold pear-shaped nucleus; and 3) the scission of the neck connecting the fragments. The multitude of final states is formed at this last step. At the intermediate cold step the nucleus may be in only one or at most a few internal states. Such states, which have definite quantum numbers for all degrees of freedom except the motion across the barrier, are called fission channels [31].

At the cold step the nucleus is a pear-shaped top. The spectrum of such a system looks as follows [31]. For a fixed internal state $|a, K\rangle$ (K is the projection of the total angular momentum J onto the axis of the top), there is a band of rotational states. If $K \neq 0$, then there are two rotational levels of opposite parity ($\eta = \pm 1$) for each value of J . For $K = 0$ the parity is related to J unambiguously: $\eta = (-1)^J \chi$ (the internal parity), so that for each J there is only a single level. The wave function of the rotating nucleus may be written as follows

$$|a, K\rangle_{JJ_z}^{\eta} = \frac{1}{\sqrt{2}} \left[|a, K, J, J_z\rangle + \eta |a, \bar{K}, J, J_z\rangle \right]$$

$$|a, K, J, J_z\rangle = \sqrt{\frac{2J+1}{4\pi}} \left(\mathcal{D}_{J_z, K}^J(\varphi, \theta, 0) \right)^* |a, K\rangle \quad (26)$$

$$|a, \bar{K}, J, J_z\rangle = (-1)^{J+K} |a, -K, J, J_z\rangle$$

Experimentally, the excitation energy of a nucleus is specified very accurately, within $\delta E \sim 0.03$ eV, which is the thermal spread of the neutron energy. In this case it is meaningless to speak in terms of a tempo-

ral resolution of the fission process into sequential steps, since the uncertainty relation $\delta t \delta E \geq \hbar$ tells us that under the condition $\delta E < \Gamma$ the uncertainty in the time satisfies $\delta t > T$, where T is the lifetime of the nucleus. In this situation the fission process one should describe by a wave function $\psi(E)$ corresponding to a fixed energy. Such a wave function incorporates parts corresponding to both the initial compound nucleus and the cold step.

Let us consider the amplitude of transition from initial state $|in\rangle$ to the intermediate cold state $|a\rangle$. This amplitude is represented by the graph shown at fig.7, more precisely its part before the circle (the circle corresponds to the cold state). For the capture of the s-wave neutron

$$\langle a|in\rangle = -\frac{1}{2p} \sum_{s\text{-res.}} \frac{\langle a|\psi_s\rangle \langle \psi_s|in\rangle}{E - E_s + i\Gamma_s/2} = \quad (27)$$

$$= -\frac{1}{2p} \sum_{s\text{-res.}} C_{II_2}^{JJ_z} T_s(E) \frac{1}{E - E_s + i\Gamma_s/2} \langle a|\psi_s\rangle$$

Here ψ_s is the wave function of the compound state. We take into account the explicit form of the capture amplitude $\langle \psi_s|in\rangle$ (see eq.(16)). The parity η of the cold state $|a\rangle$ is equal to the parity of ψ_s . The amplitude $\langle a|\psi_s\rangle$ describes the admixture of the cold state to the wave function of compound nucleus. We can say that $|a\rangle^{\eta}$ is one of the components ψ_s in decomposition(3).

The parity nonconservation arises due to the diagram shown at fig.8 [15, 16]. The transition amplitude to the cold state

$$\langle a|in\rangle = -\frac{1}{2p} \sum_{s,p\text{-res.}} \frac{\langle a|\psi_p\rangle \langle \psi_p|H_w|\psi_s\rangle \langle \psi_s|in\rangle}{(E - E_p + i\Gamma_p/2)(E - E_s + i\Gamma_s/2)} = \quad (28)$$

$$= -\frac{1}{2p} \sum_{s,p\text{-res.}} C_{II_z}^{J J_z} \frac{T_s(E)}{E-E_s+i\Gamma_s/2} \bar{\eta} \langle a | \psi_p \rangle \frac{\langle \psi_p | H_w | \psi_s \rangle}{E-E_p+i\Gamma_p/2}$$

Here $\bar{\eta} = -\eta$ is the parity of the p-wave resonance. We consider the case of one fission channel with $K \neq 0$, therefore for fixed internal state $|a\rangle$ there are two rotational states of opposite parity. Using eqs.(27),(28) it is easy to find the wave function at cold step

$$|\tilde{a}\rangle = |a\rangle^{\eta} \langle a | \psi_s \rangle + |a\rangle^{\bar{\eta}} \langle a | \psi_p \rangle =$$

$$= -\frac{1}{2p} \left(C_{II_z}^{J J_z} \frac{T_s}{E-E_s+i\Gamma_s/2} \langle a | \psi_s \rangle [|a\rangle^{\eta} + \beta |a\rangle^{\bar{\eta}}] \right) \quad (29)$$

$$\beta = \frac{\langle \psi_p | H_w | \psi_s \rangle \langle a | \psi_p \rangle}{E-E_p+i\Gamma_p/2 \langle a | \psi_s \rangle} \sim 10^{-4}$$

For simplicity we consider here the case of one s-resonance and one p-resonance. For numerical estimation we use (9) and take into account that fission amplitudes for s- and p-resonance are the same order of magnitude: $\langle a | \psi_p \rangle \sim \langle a | \psi_s \rangle$. Thus the mixing of opposite parity rotational states of cold nucleus has the same order of magnitude as mixing of compound states. It is obvious from eq.(29) that for large neutron energy spread $\delta E \gg D$ the PNC-mixing of cold states is suppressed by a factor $\sqrt{\delta E/D}$ due to the random sign of amplitudes corresponding to different s- and p-resonances. In this case the temporal description is possible and the suppression of PNC-effect corresponds usual statement that at cold step the nucleus due to the complicated dynamics "forget" the initial compound state.

At scission the K is conserved. Let us suppose that parity is conserved at scission as well. It is very reason-

nable supposition because here we talk about the motion of almost macroscopic fragments. In this case the wave function of angular motion of fragments coincides with the angular part of cold nucleus wave function. According to eq.(29)

$$\psi_{z \rightarrow \infty} \sim C_{II_z}^{J J_z} \left[|a_K\rangle^{\eta} + \beta |a_K\rangle^{\bar{\eta}} \right] \quad (30)$$

Squaring ψ and averaging over the polarization of the target nucleus we find the angular distribution of the fragments with respect the polarization of initial neutron.

$$w(\theta) = 1 + a \cos \theta \quad (31)$$

$$a = 2 \operatorname{Re} \beta \times \frac{K}{I+1/2} (-1)^{J-I-1/2} \sim 10^{-4}$$

The estimation is in accordance with the experimental data^[5].

The above example concerns the ideal case of one s- and one p-resonance and one fission channel with $K \neq 0$. The formulae for the general case are very cumbersome and we do not present them here. However we wish to emphasize the following point. If $K = 0$, the cold nucleus has no rotational levels of different parity and identical J . Nevertheless because of the interference of neutron resonances with different J the effect does not vanish. To demonstrate this assertion, we consider the particular case of the reaction $^{239}\text{Pu}(n, f)$ ($I = 1/2$). The thermal neutrons are captured into the 10^+ and 11^+ resonances. With $K = 0$, the parity of the cold nucleus is $\eta = (-1)^J$, so that fission is allowed from the 0^+ resonance, while fission from the 1^+ through a channel with $K = 0$ is forbidden. The weak interaction, however, admixes the

$|1^- \rangle$ compound state to $|1^+ \rangle$ state, and fission from $|1^- \rangle$ is possible. Therefore at cold step of fission the function Y_{1m} is admixed to Y_{00} , and this is the PNC effect.

In conclusion we want to say a few words about the P-even angular correlations: $\vec{p}_f \vec{p}$ and $\vec{p}_f [\vec{p} \times \vec{\sigma}]$ ($\vec{\sigma}$ and \vec{p} are the spin and momentum of the neutron, and \vec{p}_f is the momentum of the light fragment). From both the experimental and theoretical standpoints, these correlations are intimately related to PNC in fission^[32,33,34]. The P-even correlations arise due to the interference of diagrams presented at fig.7 and fig.9. For the non resonant neutrons the magnitude of the P-even correlations is of the order of $\sim pR$ (R is the nucleus radius). For thermal neutrons $pR \sim 3 \cdot 10^{-4}$. This estimation is in agreement with the experimental data, compilation of which is presented in ref.^[5].

We wish to emphasize that the investigation of correlations $\vec{p}_f \vec{p}$ and $\vec{p}_f [\vec{p} \times \vec{\sigma}]$ is effective way to search the p-wave resonances in ^{239}Pu . The ^{239}Pu is convenient because it has relatively narrow resonances. For neutron energy $E_n \sim 1 - 10$ eV the expected magnitude of P-even correlation in p-resonance is 1 - 10%.

References

1. Yu.G.Abov, P.A.Krupchitsky and Ya.A.Oratovsky. Phys. Lett. 12 (1964) 25.
2. Yu.G.Abov and P.A.Krupchitsky. Usp. Fiz. Nauk 118 (1976) 141 [Sov. Phys. Usp. 19 (1976) 75].
3. G.V.Danilyan et al. Pis'ma Zh. Eksp. Teor. Fiz. 26 (1977) 197 [JETP Lett. 26 (1977) 186].
4. G.V.Danilyan. Usp. Fiz. Nauk 131 (1980) 329 [Sov. Phys. Usp. 23 (1980) 445].
5. P.A.Krupchitsky. Fundamental Research with Polarized Slow Neutrons. Energoatomizdat, Moscow, 1985 (Engl. transl. Springer-Verlag, 1987).
6. M.Forte et al. Phys. Rev. Lett. 45 (1980) 2088.
7. E.A.Kolomensky et al. Phys. Lett. B107 (1981) 272.
8. V.P.Alfimenkov et al. Pis'ma Zh. Eksp. Teor. Fiz. 34 (1981) 308.
9. V.P.Alfimenkov. Usp. Fiz. Nauk 144 (1984) 361 [Sov. Phys. Usp. 27 (1984) 690].
10. R.Haas, L.B.Leipuner and R.K.Adaire. Phys. Rev. 116 (1952) 1221.
11. R.L.Blin-Stoile. Phys. Rev. 120 (1960) 181.
12. I.S.Shapiro. Usp. Fiz. Nauk 95 (1968) 647. [Sov. Phys. Usp. 11 (1969) 582].
13. A.Bohr and B.R.Mottelson. Nuclear Structure, vol. 1. Benjamin, New York, 1969.
14. S.G.Kadmensky, V.P.Markushev and V.I.Furman. Yad. Fiz. 31 (1980) 1175.
15. V.V.Flambaum and O.P.Sushkov. Phys. Lett. B94 (1980) 277; Yad. Fiz. 33 (1981) 59 [Sov. J.Nucl. Phys. 33 (1981) 31].
16. O.P.Sushkov and V.V.Flambaum. Usp. Fiz. Nauk 136 (1982) 3 [Sov. Phys. Usp. 25 (1982) 1].
17. S.G.Kadmensky, V.P.Markushev and V.I.Furman. Yad. Fiz. 37 (1983) 581.
18. V.V.Flambaum and O.P.Sushkov. Nucl. Phys. A412 (1984) 13.
19. F.C.Michel. Phys. Rev. 133 (1964) 329.
20. L.Stodolsky. Phys. Lett. B50 (1974) 352.
21. M.Forte. ILL Research Proposal 03-03-002, 1976.
22. M.Forte. Inst. Phys. Conf. Ser. No42, 1978, Ch.2, p.86.
23. O.P.Sushkov and V.V.Flambaum. Pis'ma Zh. Eksp. Teor. Fiz. 32, (1980) 377. [JETP Lett. 32 (1980) 355].
24. V.E.Bunakov and V.P.Gudkov. Z. Phys. A303 (1981) 285.
25. V.E.Bunakov and V.P.Gudkov. Nucl. Phys. A401 (1983) 93.

- 26. D.F.Zaretsky and V.K.Sirotkin. Yad. Fiz. 37 (1983)607.
- 27. D.F.Zaretsky and V.K.Sirotkin. Yad. Fiz. 39 (1984)585.
- 28. S.Noguera and B.Desplanques. Nucl. Phys. A457 (1986) 189.
- 29. V.A.Vesna et al. Pis'ma Zh. Eksp. Teor. Fiz. 35 (1982) 351.
- 30. V.P.Alfimenkov et al. Pis'ma Zh. Eksp. Teor. Fiz. 35 (1982) 42; Nucl. Phys. A398 (1983) 93.
- 31. A.Bohr and B.R.Mottelson. Nuclear Structure, vol.2. Benjamin, New York, 1974.
- 32. V.A.Vesna et al. Pis'ma Zh. Eksp. Teor. Fiz. 31 (1980) 704 [JETP Lett. 31 (1980) 663].
- 33. A.K.Petukhov et al. Pis'ma Zh. Eksp. Teor. Fiz. 32 (1980) 324 [JETP Lett. 32 (1980) 300].
- 34. O.P.Sushkov and V.V.Flambaum. Yad. Fiz. 33 (1981) 629 [Sov. J. Nucl. Phys. 33 (1981) 329].

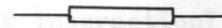


Fig. 1



Fig. 2



Fig. 3

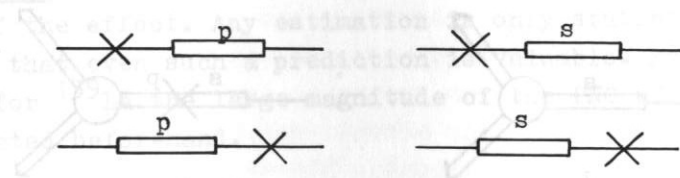


Fig. 4

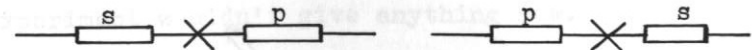


Fig. 5

26. D.F.Zaretsky and V.K.Sirotkin. *Yad. Fiz.* **37** (1983)607.
 27. D.F.Zaretsky and V.K.Sirotkin. *Yad. Fiz.* **38** (1984)585.
 28. S.Noguera and Desplanches. *Nucl. Phys.* **A197** (1974) 189.
 29. V.A.Vechny et al. *Fiz. Ya. Zh. Exp. Teor. Fiz.* **22** (1982) 351.
 30. V.P. Filin et al. *Fiz. Ya. Zh. Exp. Teor. Fiz.* **42** (1980) 421.
 31. A. Bohr. *Nuclear Structure*. Benjamin, New York, 1974.
 32. V.A.Vechny et al. *Fiz. Ya. Zh. Exp. Teor. Fiz.* **70** (1984) 704.
 33. A.K.Petukhov et al. *Fiz. Ya. Zh. Exp. Teor. Fiz.* **32** (1980) 324.
 34. O.Sushkov and V.V. ... *Fiz. Ya. Zh. Exp. Teor. Fiz.* **33** (1981) 330.

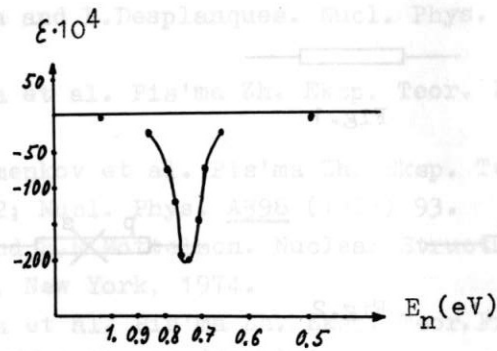


Fig.6

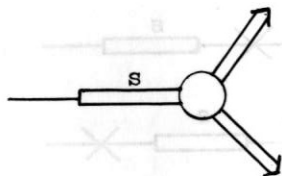


Fig.7

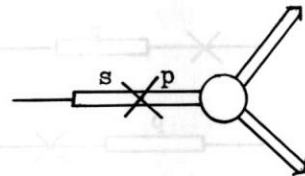


Fig.8

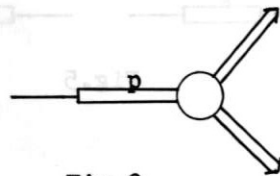


Fig.9

DISCUSSION

G.Soff: I didn't quite understand which precise quantity you ultimately want to deduce? Do you want to learn something about weak interaction?

O.Sushkov: I do not think that we can learn very much about weak interaction because of complicated structure of a compound nucleus. However we learn very much about the structure of a compound nucleus and in general about the small effects in any stochastic quantum system. The second lesson is that we understand now that a compound nucleus is suitable for the search of PT-violation and maybe for the test of quantum mechanics.

P.Vogel: Can you predict beforehand whether the PNC effect on a given p-wave state will be very large (as in ^{139}La)?

O.Sushkov: Of course, we can not predict the precise value of the effect. Any estimation is only statistical. I think that even such a prediction is valuable. By the way, just for ^{139}La the large magnitude of the PNC effect was predicted beforehand.

Yu.A.Aleksandrov: Are there the experiments on the test of PNC in the neutron diffraction at the Bragg peak?

O.Sushkov: Such an experiment was suggested by Forte but it was not carried out. I think that in present situation this experiment wouldn't give anything new.

T- AND P-ODD NUCLEAR MOMENTS

V.V. Flambaum

Institute of Nuclear Physics, 630090, Novosibirsk, USSR

Abstract

Electromagnetic nuclear moments induced by spatial and time invariance violating nuclear forces are considered. Analytic expression for P-odd anapole moment is obtained in the shell model. Analytic estimations and results of numerical calculations for T-odd moments (Electric dipole, magnetic quadrupole and Schiff moments) are presented. The electric dipole moments of the nuclei exceed that of the neutron by one to two orders of magnitude. P- and T-odd nuclear moments can be measured in atomic and molecular experiments. Limits on the anapole moment of ^{133}Cs nucleus, on the Schiff moments of ^{129}Xe and ^{205}Tl and on the constants of T-odd nucleon-nucleon interaction have been obtained already.

Nuclear moments induced by nuclear forces violating spatial (P) and time (T) parity, are considered in this review. Simplest moment is the electric dipole moment (EDM)

$$\vec{d} = e \int \vec{r} \rho d^3r = d \frac{\vec{I}}{I} \quad (1)$$

where $e \delta \rho$ is the correction to charge density induced by P + T-odd nucleon-nucleon interaction, e is proton charge, I is nuclear spin.

However, EDM of pointlike nucleus is shielded by electrons in a neutral atom (Schiff's theorem^[1]). Schiff's theorem reduces to the fact that P- and T-odd potential of the nucleus should be written in the form

$$\delta \varphi(\vec{R}) = e \int \frac{\delta \rho(\vec{r}) d^3r}{|\vec{R} - \vec{r}|} + \frac{1}{Z} (\vec{d} \cdot \vec{\nabla}) \int \frac{\rho_c(r) d^3r}{|\vec{R} - \vec{r}|} \quad (2)$$

where $\rho_c(r)$ is the spherically symmetric part of nuclear charge density, $\int d^3r \rho_c(r) = Z$. The second term in (2) ensures in accord with Schiff's theorem, the vanishing of the dipole term of the expansion of the potential outside the nucleus. There are two irreducible tensors in the following order of expansion of $\delta \varphi(\vec{R})$ in powers of R^{-1}

$$\delta \varphi(\vec{R}) = -\vec{Q} \cdot \vec{\nabla} \Delta \frac{1}{R} + O_{mng} \nabla_m \nabla_n \nabla_g \frac{1}{R} \quad (3)$$

Second term is the octupole moment field, first term is, in fact, the dipole electric field inside the nucleus. First term gives larger contribution to atomic and molecular EDM. Interaction of electrons with Q is of the form

$$H_{TP} = -e \delta \varphi = 4\pi e \vec{Q} \cdot \vec{\nabla} \delta(\vec{R})$$

$$Q = \frac{1}{10} \left[e \int \rho \vec{r} r^2 d^3r - \frac{5}{3} \vec{d} r_g^2 \right] = Q \frac{\vec{I}}{I} \quad (4)$$

where r_g^2 is the mean squared charge radius of the nucleus. We shall here after call \vec{Q} the Schiff Moment (SM) of the nucleus.

A T- + P-parity nonconserving interaction between

electron and nucleus can be caused also by the nuclear magnetic quadrupole moment (MQM). Besides MQM, P-odd anapole moment of nucleus appears in multipole expansion of vector-potential:

$$A_i(\vec{R}) = \int \frac{j_i(\vec{z}) d^3z}{|\vec{R} - \vec{z}|} = - \int j_i z_m d^3z \nabla_m \frac{1}{R} + \frac{1}{2} \int j_i z_m z_n d^3z \nabla_m \nabla_n \frac{1}{R} + \dots \quad (5)$$

j is the electromagnetic current density of the nucleons,

$$\vec{j} = - \frac{ieq}{2m} [\psi^* \vec{\nabla} \psi - (\vec{\nabla} \psi^*) \psi] + M \frac{e}{2m} \vec{\nabla} \times (\psi^* \vec{\sigma} \psi)$$

First term of expansion is the field of magnetic moment, second term can be reduced to two irreducible tensors

$$A_i(\vec{R}) = a_c \delta(\vec{R}) - \frac{1}{6} \epsilon_{ien} M_{nk} \nabla_e \nabla_k \frac{1}{R} \quad (6)$$

a - anapole, M - magnetic quadrupole.

$$\vec{a} = \frac{\pi e}{2m} \left\langle \sum_1^A 2M(\vec{\sigma} \times \vec{\sigma}) - q(\vec{p} z^2 + z^2 \vec{p}) \right\rangle = a \frac{\vec{I}}{I} \quad (7)$$

$$M_{nk} = \frac{e}{2m} \left\langle \sum_1^A 3M(z_n z_k + z_k z_n - \frac{2}{3} \vec{z} \vec{z} \delta_{nk}) + 2q(z_k l_n + z_n l_k) \right\rangle$$

$$= \frac{3}{2} \frac{M}{I(2I-1)} \left[I_n I_k + I_k I_n - \frac{2}{3} I(I+1) \delta_{nk} \right] \quad (8)$$

Contact current $\vec{j}_c = ie[w, \vec{z}]$ (see(9)) contributes also to \vec{a} . Here the summation is taken over nucleons of the nucleus,

A is the number of nucleons, $M \frac{e}{2m}$ is nucleon magnetic moment, $q = 1$ for proton and $q = 0$ for neutron, \vec{p} , \vec{l} are momentum and angular momentum of a nucleon.

We have considered only several lowest P- and T-odd multipoles. It is interesting to find their total number with fixed spin I . The classification of electromagnetic

form-factors was first presented in Ref. [2] using a transition into the annihilation channel. The total number of invariant form-factors that conserve (+) and violate (-) the P, T and C invariances are presented in the table. If two quantities are contained in one line of the table, the left and right quantities pertain to integer and half-integer spin respectively. The total number of electromagnetic form-factors is $6I + 1$.

Note that the field of all P-odd and T-even moments is contact (proportional to $\delta(\vec{R})$) similar to the field of anapole moment which is the lowest multipole of such type. As for the T-odd multipoles here only P-even moments have contact field. Finally, all C-odd moments have contact field [3].

P	T	C	Number of form-factors	Field
+	+	+	$2I + 1$	long-range
-	+	-	$I \quad I+1/2$	contact
+	-	-	$I \quad I-1/2$	contact
-	-	+	$2I$	long-range

Simple derivation of the results presented in the table and complete list of references can be found in Ref. [4].

It is interesting that interaction coupled to P-odd polarizability (P-odd Van der Waals forces) is not contact and decreases outside the nucleus as $(\vec{I}_1 \times \vec{I}_2) \vec{R} / R^6$ [5]. But in practice this interaction is small since it corresponds to two-photon exchange.

Let us turn to the calculation of P- and T-odd moments. We shall use in our calculation the simple shell model of a nucleus. Unpaired valence nucleon gives main contribution to the anapole moment [6]. The parity violating weak

interaction of the external nucleon with the core nucleons in heavy nucleus is described by the Hamiltonian

$$W = \frac{G}{\sqrt{2}} \frac{g}{2m} \{ \vec{\sigma} \vec{p} \rho(\vec{r}) + \rho(\vec{r}) \vec{\sigma} \vec{p} \} \quad (9)$$

Here $G = 10^{-5} / m^2$ is the Fermi constant of weak interaction, $\rho(\vec{r})$ is the nuclear density ($\int d^3r \rho(\vec{r}) = A$). The dimensionless constant g can be expressed in terms of the constants of weak meson-nucleon interaction. Using the "best values" of these constants¹⁷ we have found that $g_p = 4.6$ for proton and $|g_n| \approx 1$ for neutron. Smallness of g_n is due to the cancellation of π - and ρ -contributions.

We start from a simple model leading to an analytical expression for the anapole moment of a heavy nucleus. We assume in the formula (9) the density $\rho(\vec{r})$ as a constant coinciding with the average nuclear density $\bar{\rho}$. This approximation is quite reasonable in the case of the wave function of valence nucleon being localized mainly inside the nucleus. In this approximation the solution of the Schrodinger equation

$$\left[-\frac{1}{2m} \Delta + U(r) + W \right] \Psi = E \Psi \quad (10)$$

to the first order in the perturbation W is found in an elementary way:

$$\begin{aligned} \Psi(\vec{r}) &= \exp \left\{ -i \frac{Gg\bar{\rho}}{\sqrt{2}} \vec{\sigma} \vec{r} \right\} \psi_0(\vec{r}) \approx \\ &\approx \left\{ 1 - i \frac{Gg\bar{\rho}}{\sqrt{2}} \vec{\sigma} \vec{r} \right\} \psi_0(\vec{r}) \end{aligned} \quad (11)$$

Here $\psi_0(\vec{r})$ is the unperturbed wave function. One could suspect that the interaction (9) at $\rho(\vec{r}) = \bar{\rho} = \text{const}$, being equivalent to the electromagnetic interaction with

the constant vector potential $\vec{A} = -\frac{Gg\bar{\rho}}{c\sqrt{2}} \vec{\sigma}$, should not lead to any physical consequences at all. And indeed, the orbital contribution to \vec{a} vanishes in this approximation. However, the spin contribution to (7) is quite operative even in this approximation, due to non-commutativity of β -matrices. Simple calculation with formulae (7, 11) lead to the following expression:

$$\vec{a} = \frac{Gg\bar{\rho}}{\sqrt{2}} \frac{2\pi eM}{m} \frac{K \vec{I}}{I(I+1)} \langle r^2 \rangle \quad (12)$$

$$K = (I + \frac{1}{2}) \cdot (-1)^{I + \frac{1}{2} - l}$$

The mean square radius of the valence nucleon $\langle r^2 \rangle$ is known to coincide to good accuracy with the square of the nuclear charge radius $r_g^2 \approx \frac{3}{5} r_0^2 A^{2/3}$ ($r_0 = 1.15 \text{ fm}$). Then with $\bar{\rho} = (\frac{4\pi}{3} r_0^3)^{-1}$ we get the following result¹⁶:

$$\vec{a} = \frac{Gg}{\sqrt{2}} \frac{g}{10} \frac{eM}{m r_0} A^{2/3} \frac{K \vec{I}}{(I+1)I} \quad (13)$$

The dependence of anapole moment on the atomic number A is quite natural. In the very first paper¹⁸ where the notion of an anapole moment was introduced, it was mentioned to correspond to the magnetic field configuration created by a toroidal winding (in the nucleus a toroidal spin current due to the spin-dependent phase of the wave function (11) "works"). Clearly the magnitude of anapole moment should be proportional to the magnetic flux, i.e. to the torus cross-section. This gives the dependence on $\langle r^2 \rangle$ in the formula (12) and on $A^{2/3}$ in the formula (13).

Note that the approximation (11) for the wave function allows also to find explicit expressions for higher P-odd multipoles.

Hamiltonian of magnetic interaction between relativis-

tic electron and nuclear anapole moment is

$$e \vec{\mathcal{A}} = e \vec{\mathcal{A}} s(\vec{R}) = \frac{G}{\sqrt{2}} \frac{\kappa \vec{I} \vec{\mathcal{A}}}{I(I+1)} \chi_a s(\vec{R})$$

$$\chi_a = \frac{g}{10} g \frac{\Delta M}{m \gamma_0} A^{2/3} \quad (14)$$

Here $\vec{\mathcal{A}}$ denotes the Dirac matrices, $\mathcal{A} = e^2 = 1/137$.

In a heavy nucleus with unpaired proton dimensionless constant $\chi_a \sim 0.3$. We have also carried out more accurate numerical calculations with realistic density and with the use of the Saxon-Woods potential, including spin-orbit coupling, for the calculation of wave function and Green function of valence nucleon. Results agree with formulae (12), (13), (14) within an accuracy of 10-30%. It is possible to give a formula which fits the results of numerical calculations for nondeformed nuclei with an accuracy better than 10%^[6].

$$\chi_a = \frac{g}{10} g \frac{\Delta M}{m \gamma_0} A^{2/3} \left\{ 1 - \frac{5\lambda [\lambda I(I+1) + \frac{1}{2} - \kappa]}{6 A^{2/3} \gamma_0^2} \right\} \quad (15)$$

$\lambda = 0.37 \text{ fm}^2$ is the constant of spin-orbit interaction.

Note that weak interaction of neutral currents (of electron vector current and nucleon axial current) leads to the Hamiltonian which is similar to (14). However, the constant of this interaction is small: $\chi_2 = 1.25(\frac{1}{2} - 2 \sin^2 \theta_w) \approx 0.05 \ll \chi_a \sim 0.3$, θ_w is Weinberg angle.

Let us now discuss the possibilities to detect anapole moment. Many effects of parity nonconservation in atoms, molecules and crystals that depend on nuclear spin have been discussed (see, e.g. book^[9]). As it was shown above, nuclear anapole moment gives the dominant contribution to these effects. Firstly, interaction (14) leads to the

difference of P-odd effects at different hyperfine components of optical transitions in heavy atoms^[10]. In the experiment of this type^[11] the limit on the anapole moment of nucleus ^{133}Cs was obtained: $\chi_a = -1.8 \pm 1.8$. The possibilities to detect anapole moment in radiofrequency atomic experiments was also discussed^[12-14]. The possibility to measure anapole moments in the experiments with diatomic molecules seems realistic. In molecules nuclear-spin-dependent P-odd interaction (14) is enhanced by 10^4-10^5 due to mixing of very close molecular rotational levels of opposite parity^[15-17].

Thus the detection of nuclear anapole moment is an extremely interesting problem lying at the frontier of the modern experimental facilities. The measurement of anapole moments would give a unique information on the P-odd interaction potential between nucleon and heavy nucleus.

Let us return to T-odd nuclear moments. Hamiltonian of T + P-odd interaction of valence nucleon with a nucleus is

$$W_{TP} = \frac{G}{2\sqrt{2}m} \eta \vec{\mathcal{A}} \vec{\nabla} \rho \quad (16)$$

Here η is dimensionless constant characterizing the strength of the interaction. Radius of strong nucleon-nucleon interaction (similar to the weak one) is small. Therefore the strong potential $u(\vec{r})$ and nuclear density $\rho(\vec{r})$ shapes are quite similar. Assuming that they coincide: $\rho(\vec{r}) = u(\vec{r}) \cdot [\rho(0)/u(0)]$, we can rewrite (16) in the form

$$W_{TP} = - \xi \vec{\mathcal{A}} \vec{\nabla} u(\vec{r})$$

$$\xi = - \eta \frac{G}{2\sqrt{2}m} \frac{\rho(0)}{u(0)} = 2 \cdot 10^{-21} \eta [\text{cm}] \quad (17)$$

The total potential in which the nucleon moves is, correspondingly,

$$\tilde{U} = U + W_{TP} = U(\vec{r}) - \xi \vec{\sigma} \nabla U(\vec{r}) \approx U(\vec{r} - \xi \vec{\sigma}) \quad (18)$$

It is clear hence that the wave function, with W_{TP} taken into account, is of the form

$$\tilde{\Psi} = \Psi_0(\vec{r} - \xi \vec{\sigma}) = (1 - \xi \vec{\sigma} \nabla) \Psi_0(\vec{r}) \quad (19)$$

where $\Psi_0(\vec{r})$ is the unperturbed wave function. It is clear that the state $\tilde{\Psi}$ with shifted centre (shift is $\xi \langle \vec{\sigma} \rangle$) has nonzero dipole moment. With the aid of (19) as well as (1), (4), (8) we obtain the contributions of valence nucleon to T-odd moments^[18]:

$$d = e(q - \frac{Z}{A}) \xi \langle \vec{\sigma} \rangle, \quad (20)$$

$$Q = \frac{e q}{10} \xi \left[\langle \vec{\sigma} \rangle + \frac{1}{I+1} \langle r^2 \rangle - \frac{5}{3} \langle \vec{\sigma} \rangle r^2 \right] \approx e q \left[\langle \vec{\sigma} \rangle - \frac{3}{2(I+1)} \right] A^{2/3} \cdot 10^{-9} \eta \text{ [fm}^3 \text{]} \quad (21)$$

$$M = -\frac{e}{m} (N-1)(2I-1) \langle \vec{\sigma} \rangle \xi \quad (22)$$

In the shell model

$$\langle \vec{\sigma} \rangle = \frac{\frac{1}{2} - K}{I+1} = \begin{cases} 1, & I = l + \frac{1}{2} \\ -\frac{I}{I+1}, & I = l - \frac{1}{2} \end{cases}$$

In the dipole moment there is effective charge $e(q - \frac{Z}{A})$ rather than eq , due to recoil of nuclear core (similar to E1-transitions).

Besides the considered mechanism, another mechanism gives contribution to T-odd moments. Valence nucleon po-

larizes nuclear core by T-odd field. As a result T-odd moments appear in the charge and current density of core nucleons. It is possible to show analytically in the oscillator model of the nucleus that the contribution of the second mechanism is comparable with the contribution of the first mechanism^[19]. For example, second mechanism simply redefines constant eq in EDM (20). Contribution of the second mechanism to the anapole moment is smaller than that of the first mechanism.

The real calculation of Schiff moments for the Xe, Hg and Tl nuclei, that are now of experimental interest, was performed by us^[19] using Saxon-Woods potential with spin-orbit correction. The following values were obtained (in units $10^{-8} \text{ e} \cdot \text{fm}^3$):

¹⁹⁹ Xe	¹³¹ Xe	¹⁹⁹ Hg	²⁰¹ Hg	^{203,205} Tl
$1.75 \eta_{np}$	$-2.6 \eta_{np}$	$-1.4 \eta_{np}$	$2.4 \eta_{np}$	$(1.2 \eta_{pp} - 1.4 \eta_{pn})$

In the first four nuclei the non-paired nucleon is neutron, therefore the Schiff moment is caused by the polarization of core proton density and can be expressed through the constant η_{np} . In thallium the contribution of the core protons $1.23 \eta_{pp}$ is comparable with the valence proton contribution ($-1.4 \eta_{pn} - 0.04 \eta_{pp}$). Constants η_{ab} are defined in the Hamiltonian of T+P-odd nucleon-nucleon interaction:

$$W_{ab} = \frac{G}{\sqrt{2} 2m} \left((\eta_{ab} \vec{\sigma}_a - \eta_{ba} \vec{\sigma}_b) \nabla_a \delta(\vec{r}_a - \vec{r}_b) + \eta'_{ab} \vec{\sigma}_a \times \vec{\sigma}_b \left\{ (\vec{P}_a - \vec{P}_b) \delta(\vec{r}_a - \vec{r}_b) + \delta(\vec{r}_a - \vec{r}_b) (\vec{P}_a - \vec{P}_b) \right\} \right) \quad (16a)$$

This Hamiltonian reduces to (16) after averaging over core nucleons.

Thus, the scale of all T-odd moments is determined

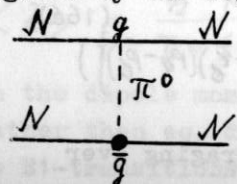
by the constant ξ which has the dimension of length:

$$d \sim e \xi, \quad Q \sim e \xi^2 / 10, \quad M \sim \frac{e}{m} \xi, \quad \text{etc.}$$

T- and P-odd moments could be enhanced if there is nuclear level of opposite parity with the same angular momentum close to the ground state^[20-22, 18] (according to perturbation theory $d, Q, M, a \sim \langle +|W| - \rangle / (E_+ - E_-)$). This situation occurs in deformed nuclei. Unfortunately, if only heavy stable nuclei are considered, the choice is quite poor. We have ^{161}Dy ($E_+ - E_- = 26$ keV), ^{237}Np ($E_+ - E_- = 60$ keV) and also ^{153}Eu , ^{155}Gd , ^{163}Dy , ^{233}U ($E_+ - E_- \sim 100$ keV). At first glance one might expect considerable enhancement of the effects compared with spherical nuclei, for which $\Delta E \sim 8$ MeV. It turns out, however, that the enhancement hardly exceeds 10 in these nuclei. The reasons are discussed in Ref.^[18]

Besides T-odd nuclear forces, EDM of valence nucleon also gives contribution to T-odd nuclear moments (see, e.g. book^[9] and papers^[21, 23]). To find the dominant mechanism it is necessary to compare nuclear EDM induced by T-odd nuclear forces and nucleon EDM. Besides that this comparison allows us to estimate the significance of atomic and molecular experiments since the experiments on neutron EDM have been the most advanced up to now.

We shall use simplest one-boson exchange model. The largest contribution to the constant η is probably given by the lightest π^0 -meson:

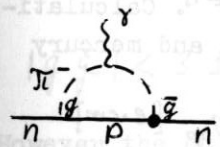


$$\frac{G}{\sqrt{2}} \eta \approx - \frac{g \bar{g}_0}{m_\pi^2} \quad (23)$$

Here g and \bar{g} are the constants of strong and T-odd interactions of π -meson and nucleon:

$$(g i \bar{n} \gamma_5 n + \bar{g}_0 \bar{p} p) \pi^0 + \sqrt{2} (g i \bar{p} \gamma_5 n + \bar{g}_- \bar{p} n) (\pi^-)^+ + \dots \quad (24)$$

The neutron EDM is given by the loop diagram^[24]



$$d_n = \frac{e g \bar{g}_-}{4 \pi^2 m} \ln \frac{M}{m_\pi} \quad (25)$$

Here $M \sim m_p \sim 700$ MeV is the scale at which π -meson loop converges. The values of η and d_n are expressed generally speaking in terms of different quantities \bar{g}_0 and \bar{g}_- , respectively. But, e.g., in the model of T-invariance violation with the θ -term $|g \bar{g}_0| = |g \bar{g}_-| = 0.36 |\theta|$ ^[24]. Comparing (17), (23) with (25) we find^[18, 19]

$$\frac{d}{d_n} \sim \frac{e \xi}{d_n} \sim 2 \pi (m_\pi^2 \xi^3 |U(0)|)^{-1} \sim 40 \quad (26)$$

Thus, nuclear EDM exceeds nucleon EDM by one to two orders of magnitude. Analogously T-odd nuclear forces give $e \xi / d_n \sim 10-100$ times larger contributions to all T-odd nuclear moments. This enhancement considerably increases the significance of atomic and molecular experiments since earlier they were interpreted as the limits on proton EDM.

Interactions of electrons with Schiff moment and magnetic quadrupole moment induce EDM of atoms and molecules. Contribution of MQM is an order of magnitude larger than that of the Schiff moment^[23, 18]. However MQM "works" only in the systems with nonzero electron angular momentum where magnetic field of electrons is not zero. In the table there are several examples of atomic and molecular EDM^[18, 19, 28, 29].

Source of T-viol.	T-meson exch.	T-odd forces	SM	MQM	MQM	SM	MQM
	neutron	nucleus	Xe	Cs	¹⁶¹ Dy*	TlF	¹⁶¹ DyI
$d \cdot 10^{24} / e \cdot \text{cm}$	10-100	1000	0.05	5	700	$5 \cdot 10^3$	10^7

The most sensitive experiments are carried out with TlF molecule^[25,26] and ¹²⁹Xe and ¹⁹⁹Hg atoms^[27]. Calculations^[28,19] give the following values of xenon and mercury EDM:

$$d_A(^{129}\text{Xe}) = 2.7 \cdot 10^{-18} \frac{Q}{[e \cdot \text{fm}^3]} [e \cdot \text{cm}] = 4.7 \cdot 10^{-26} \eta_{np} [e \cdot \text{cm}] \quad (27)$$

$$d_A(^{199}\text{Hg}) = -4 \cdot 10^{-17} \frac{Q}{[e \cdot \text{fm}^3]} [e \cdot \text{cm}] = 5.6 \cdot 10^{-25} [e \cdot \text{cm}] \eta_{np} \quad (28)$$

Mercury EDM is larger since T- and P-odd interactions increase with nuclear charge faster than Z^2 . Using experimental limit^[27]

$$d_A(^{129}\text{Xe}) = (-0.3 \pm 1.1) \cdot 10^{-26} [e \cdot \text{cm}] \quad (29)$$

we obtain the limit on the constant of T + P-odd neutron-proton interaction^[19]

$$\eta_{np} = -0.06 \pm 0.23 \quad (30)$$

It is seen that T-odd nuclear forces are at least an order of magnitude weaker than P-odd (let us remind that P-odd constants are $g_p = 4.6$, $g_n \sim 1$). Experiment with TlF molecule^[26] gives the limit^[19]

$$1.2 \eta_{pp} - 1.4 \eta_{pn} = 0.8 \pm 1.2 \quad (31)$$

Limit (30) gives also the limits on the constant of the T-odd pion-nucleon interaction and the parameter θ :

$$|g \bar{g}_0| = (1 \pm 4) \cdot 10^{-8}, \quad |\theta| < 2.5 \cdot 10^{-7} \quad (32)$$

Limit on θ is weaker than the limit following from the neutron EDM measurement^[30]:

$$|g \bar{g}_0| < 3 \cdot 10^{-10}, \quad |\theta| < 0.8 \cdot 10^{-9}$$

However the authors of Ref.^[27] plan to increase sensitivity of atomic experiments by four orders of magnitude.

Measurements of EDM of xenon, mercury and TlF give also the limits on electron EDM, proton EDM and constants of T + P-odd electron-nucleon interactions^[21,26,28,31,32] (see table).

Thus atomic and molecular experiments are the unique source of information about T- and P-odd interactions.

T-odd interactions	$d_A(^{129}\text{Xe})$ [e·cm]	$d_A(^{199}\text{Hg})$ [e·cm]	Limits from ^{129}Xe [27]	Limits from TIF [21,26]
nucleon-nucleon $\gamma_{ab} \frac{e}{2M} \vec{\sigma}_a \vec{V}_a \delta(\vec{r}_a - \vec{r}_b)$	$4.7 \cdot 10^{-26} \eta_{np}$	$5.6 \cdot 10^{-25} \eta_{np}$	$\eta_{np} = -0.06 \pm 0.23$	$1.2 \eta_{np} - 1.4 \eta_{pn} =$ $= 0.8 \pm 1.2$
electron-nucleon $c^{sp} i \frac{e}{\sqrt{2}} \bar{N} N \vec{e} \chi_s e$	$-3.7 \cdot 10^{-23} \cdot$ $(0.4 C_p^{sp} + 0.6 C_n^{sp})$	$-4.7 \cdot 10^{-22}$ $(0.4 C_p^{sp} + 0.6 C_n^{sp})$	$0.4 C_p^{sp} + 0.6 C_n^{sp} =$ $= (0.8 \pm 2.9) \cdot 10^{-4}$	$0.4 C_p^{sp} + 0.6 C_n^{sp} =$ $= (3 \pm 5) \cdot 10^{-4}$
$c^{ps} i \frac{e}{\sqrt{2}} \bar{N} \chi_s N \vec{e} e$	$1 \cdot 10^{-23} \cdot$ $(\frac{1}{4} C_p^{ps} + \frac{3}{4} C_n^{ps})$	$6 \cdot 10^{-23} C_n^{ps}$	$\frac{1}{4} C_p^{ps} + \frac{3}{4} C_n^{ps} =$ $= (-0.3 \pm 1.1) \cdot 10^{-3}$	$\frac{3}{4} C_p^{ps} + \frac{1}{4} C_n^{ps} =$ $= (2.5 \pm 3.8) \cdot 10^{-3}$
$c^T i \frac{e}{\sqrt{2}} \bar{N} \chi_s \gamma_{\mu\nu} N$ $\cdot \vec{e} \partial_{\mu\nu} e$	$0.41 \cdot 10^{-20} \cdot$ $(\frac{1}{4} C_p^T + \frac{3}{4} C_n^T)$	$2 \cdot 10^{-20} C_n^T$	$\frac{1}{4} C_p^T + \frac{3}{4} C_n^T =$ $= (-0.7 \pm 2.7) \cdot 10^{-6}$	$\frac{3}{4} C_p^T + \frac{1}{4} C_n^T =$ $= (6 \pm 9) \cdot 10^{-6}$
electron EDM	$-0.8 \cdot 10^{-3} d_e$ [e·cm]	$-1.4 \cdot 10^{-2} d_e$ [e·cm]	$d_e = (0.4 \pm 1.4) \cdot$ $\cdot 10^{-23}$ [e·cm]	$d_e = (0.9 \pm 1.3) \cdot$ $\cdot 10^{-23}$ [e·cm]
proton EDM	$\sim 3 \cdot 10^{-6} d_p$ [e·cm]	$\sim 2 \cdot 10^{-5} d_p$ [e·cm]	$ d_p \leq 4 \cdot 10^{-21}$ [e·cm]	$d_p = (2.3 \pm 3.4) \cdot$ $\cdot 10^{-21}$ [e·cm]

References

- Schiff L.I. Phys. Rev. 132 (1963) 2194.
- Kobzarev Yu.I., Okun' L.B. and Terent'ev M.B. Pisma ZhETF 2 (1965) 466 [JETP Lett. 2 (1965) 289].
- Dolgov A.D. Pisma ZhETF 2 (1965) 494 [JETP Lett. 2 (1965) 308].
- Flambaum V.V., Khriplovich I.B. ZhETF 79 (1980) 1656 [Sov. Phys. JETP 52 (1980) 835].
- Zhizhimov O.L., Khriplovich I.B. ZhETF 82 (1982) 1026.
- Flambaum V.V., Khriplovich I.B., Sushkov O.P. Phys. Lett. B146 (1984) 367.
- Desplanques B., Donoghue J.F., Holstein B.R. Annals of Physics 124 (1980) 449.
- Zel'dovich Ya.B. ZhETF 33 (1957) 1531 [Sov. Phys. JETP 6 (1957) 1184].
- Khriplovich I.B. Parity Nonconservation in Atomic Phenomena. Moscow, Nauka, 1981.
- Novikov V.N., Sushkov O.P., Flambaum V.V., Khriplovich I.B. ZhETF 73 (1977) 802 [Sov. Phys. JETP 46 (1977) 420].
- Gilbert S.L., Wieman C.E. Phys. Rev. A34 (1986) 792.
- Novikov V.N., Khriplovich I.B. Pisma ZhETF 22 (1975) 162.
- Balakin V.E., Kozhemyachenko S.I. Pisma ZhETF 31 (1980) 326.
- Altshuler et al. Proceeding 19 LINP Winter School (Leningrad, 1984), p.91.
- Labzovsky L.N. ZhETF 75 (1978) 856.
- Sushkov O.P., Flambaum V.V. ZhETF 75 (1978) 1208. [Sov. Phys. JETP 48 (1978) 608].
- Flambaum V.V., Khriplovich I.B. Phys. Lett. A110 (1985) 121.
- Sushkov O.P., Flambaum V.V., Khriplovich I.B. ZhETF 87 (1984) 1521 [Sov. Phys. JETP 60 (1984) 873].

19. Flambaum V.V., Khriplovich I.B., Sushkov O.P. Phys. Lett. B162 (1985) 213; Nucl. Phys. A449 (1986) 750.
20. Feinberg G. Trans. N.Y. Acad. Sci., ser. II, 38 (1977) 26.
21. Coveney P.V., Sandars P.G.H. J. Phys. B16 (1983) 3727.
22. Haxton W.C., Henley E.M. Phys. Rev. Lett. 51 (1983) 1937.
23. Khriplovich I.B. ZhETF 71 (1976) 51 [Sov. Phys. JETP 44 (1976) 25].
24. Grewther R.J., Di Vecchia P., Veneziano G., Witten E. Phys. Lett. B88 (1979) 123; B91 (1980) 487.
25. Player M.A., Sandars P.G.H. J. Phys. B3 (1970) 1620.
26. Wilkening D.A., Ramsey N.F., Larson D.J. Phys. Rev. A29 (1984) 425.
27. Vold T.G., Raab F.J., Heckel B., Fortson E.N. Phys. Rev. Lett. 52 (1984) 2229.
28. Dzuba V.A., Flambaum V.V., Silvestrov P.G. Phys. Lett. B154 (1985) 93.
29. Dzuba V.A., Flambaum V.V., Khriplovich I.B. Z. Phys. D1 (1986) 243.
30. Altarev I.S. et al. Pisma ZhETF 44 (1986) 1153.
31. Martensson-Pendrill A.-M. Phys. Rev. Lett. 54 (1985) 1153.
32. Flambaum V.V., Khriplovich I.B. ZhETF 89 (1985) 1505.

Additional note

Recent experiment with molecule TlF (D.Schropp et al. Phys. Rev. Lett. 59 (1987) 991) has 5 times better accuracy than that of Ref. [26]. It leads to more stringent limits on the constants presented in the last column of the Table.

NEUTRON ELECTRIC DIPOLE MOMENT, T-ODD NUCLEAR FORCES AND NATURE OF CP-VIOLATION

V.M.Khatsymovsky, I.B.Khriplovich, A.S.Yelkhovskiy

Institute of Nuclear Physics, 630090, Novosibirsk, USSR

Abstract

Limits on the parameters of CP-violation in the system of light quarks are extracted from the experimental limits on the neutron electric dipole moment and T-odd nuclear forces. For a number of parameters these limits turn out quite comparable. It means in particular that the searches for T-invariance violation in the neutron reactions and nuclear transitions even at the level of accuracy of P-violation experiments would be as informative as the neutron EDM searches are.

Thus far CP-violation was observed only in the neutral K-meson decays¹. Although the searches for another manifestation of CP-violation - electric dipole moment (EDM) of the neutron are going on for many years, it has not been discovered up to now. However, the limits on the neutron EDM d_n obtained in these experiments have played very important role allowing one to exclude a number of the models of CP-violation. The result of the most accurate neutron experiment² is formulated by its authors as the limit at the 95% confidence level

$$|d_n/e| < 2.6 \cdot 10^{-25} \text{ cm.} \quad (1)$$

The searches for CP-violation in atoms and molecules constitute one more trend in this field. But their results look much more modest. Being interpreted in terms of the limits on the proton or neutron EDMs these results are about 4 orders of magnitude weaker than those following from the neutron experiments.

However, as pointed out in³, the gap in the physical significance between the neutron and atomic experiments diminishes essentially if one interprets the results of the latter as limits on the effective constant η of CP-odd nucleon-nucleon interaction (the definition of the constant η will be given below) rather than on the neutron or proton EDM. It was obtained in⁴ from the most accurate measurement⁵ of the ¹²⁹Xe atom EDM that

$$|\eta| < 0.5 \quad (2)$$

In the present work the operators of the lowest dimensions 5 and 6 are constructed that can describe CP-violation in the system of light quarks and the limits on the corresponding effective constants are extracted from the results (1) and (2). For some constants these limits turn out quite comparable.

We start from the enumeration of the CP-odd operators of interest. In the case of the dimension 5 they are as follows:

$$\frac{G}{\sqrt{2}} k_u^g m_p \bar{u} g \sigma_{\mu\nu} G_{\mu\nu}^a t^a \gamma_5 u = \frac{G}{\sqrt{2}} k_u^g m_p O_u^g \quad (3)$$

and

$$\frac{G}{\sqrt{2}} k_d^g m_p \bar{d} g \sigma_{\mu\nu} G_{\mu\nu}^a t^a \gamma_5 d = \frac{G}{\sqrt{2}} k_d^g m_p O_d^g \quad (4)$$

Here $G_{\mu\nu}^a$ is the field strength of gluon, g is its coupling constant, $G = 10^{-5}/m_p^2$ is the Fermi constant of

weak interaction, m_p is the proton mass. Here and below k 's are just those dimensionless constants limits on which we are interested in.

Four-quark CP-odd operators of the dimension 6 are as follows:

$$\frac{G}{\sqrt{2}} k_q i (\bar{q} \gamma_5 q) (\bar{q} q) = \frac{G}{\sqrt{2}} k_q O_q, \quad q = u \text{ or } d; \quad (5)$$

$$\frac{G}{\sqrt{2}} k_q^c i (\bar{q} \gamma_5 t^a q) (\bar{q} t^a q) = \frac{G}{\sqrt{2}} k_q^c O_q^c; \quad (6)$$

$$\frac{G}{\sqrt{2}} k_{q_1 q_2} i (\bar{q}_1 \gamma_5 q_1) (\bar{q}_2 q_2) = \frac{G}{\sqrt{2}} k_{q_1 q_2} O_{q_1 q_2}, \quad q_1, q_2 = u, d, \quad (7)$$

$$q_1 \neq q_2;$$

$$\frac{G}{\sqrt{2}} k_{q_1 q_2}^c i (\bar{q}_1 \gamma_5 t^a q_1) (\bar{q}_2 t^a q_2) = \frac{G}{\sqrt{2}} k_{q_1 q_2}^c O_{q_1 q_2}^c, \quad q_1 \neq q_2; \quad (8)$$

$$\frac{G}{\sqrt{2}} k_t \frac{1}{2} \epsilon_{\mu\nu\alpha\beta} (\bar{u} \sigma_{\mu\nu} u) (\bar{d} \sigma_{\alpha\beta} d) = \frac{G}{\sqrt{2}} k_t O_t; \quad (9)$$

$$\frac{G}{\sqrt{2}} k_t^c \frac{1}{2} \epsilon_{\mu\nu\alpha\beta} (\bar{u} \sigma_{\mu\nu} t^a u) (\bar{d} \sigma_{\alpha\beta} t^a d) = \frac{G}{\sqrt{2}} k_t^c O_t^c. \quad (10)$$

Note that in the case of identical quarks the tensor structures of the type (9), (10) are reduced by the Fierz transformation to the scalar ones (5), (6).

We define all the operators at the low normalization point $\mu = 140$ MeV where $\alpha_s(\mu) \approx 1$.

Some words on T-odd but P-even interaction. Here the

minimal dimension of effective operators equals 7. The corresponding quark-quark interaction looks as follows:

$$\frac{G}{\sqrt{2}} \frac{k}{m_p} i (\bar{q}_1 \gamma_\mu \gamma_5 q_1) \partial_\nu (\bar{q}_2 \sigma_{\mu\nu} \gamma_5 q_2); \quad (11)$$

$$\frac{G}{\sqrt{2}} \frac{k^c}{m_p} i (\bar{q}_1 \gamma_\mu \gamma_5 t^a q_1) D_\nu^{ab} (\bar{q}_2 \sigma_{\mu\nu} \gamma_5 t^b q_2), \quad (12)$$

where D_ν^{ab} is the operator of covariant differentiation in gluon field.

The experimental limits on the corresponding component of nucleon-nucleon interaction^{6,7} is several orders of magnitude weaker than (2). For that reason we do not discuss the operators above in what follows.

It should be noted that our analysis is not related to the Kobayashi-Maskawa model of CP violation. Both the neutron EDM and T-odd nuclear forces arise in this model to the second order in the Fermi constant only, and are therefore extremely small:

$$d_n/e \approx 2 \cdot 10^{-32} \text{ cm} \quad [8],$$

$$\eta \sim 5 \cdot 10^{-10} \quad [9].$$

First of all consider the CP-odd nucleon-nucleon interaction constant. We shall take into account the π^0 -exchange only. This mechanism stands out due to the large value of the strong πNN coupling constant $g_r = 13.5$ and the smallness of the π -meson mass m_π . As for the derivative occurring at one of the vertices (here at the strong one) it arises inevitably in the case of a P-odd interaction and does not lead to a relative suppression of the corresponding contribution. Finally, a charged partic-

le exchange is suppressed as compared with that of a neutral one in the shell model of nucleus^{3,4}. Thus, the π^0 -exchange leads to the effective nucleon-nucleon interaction of the kind $\eta \frac{G}{\sqrt{2}} i (\bar{N} \gamma_5 N) (\bar{N}' N')$ with dimensionless constant

$$\eta = \frac{\sqrt{2}}{G} \frac{\tilde{g} g_r}{m_\pi^2} \quad (14)$$

Here \tilde{g} is the CP-odd πNN coupling constant. In what follows we consider CP-violating interaction between neutron and proton: $N = n$, $N' = p$, since the limit (2) corresponds in fact just to the constant of such interaction⁴.

To get the limits on the CP-odd interaction constants we use the factorization of matrix elements and the QCD sum rules technique. The calculations can be found elsewhere⁹. Here we present the results only. They are collected in Table 1. In it by ^{a)} we mark the results obtained by the sum rules method. They are less accurate than the results obtained by factorization. By ^{b)} we mark order-of-magnitude estimates that refer to the cases when only the charged pion exchange is operative.

Note that in a number of cases the limits following from the measurement of the EDM of ^{129}Xe atom are comparable to the neutron experiment limits. The gain is due not only to the specific nuclear enhancement factor pointed out in³ that allowed to extract quite meaningful limit (2) from the atomic experiment. The present consideration shows the important role of the factors arising at elementary particles level, such as the strong πNN constant $g_r = 13.5$; chiral enhancement factor $\sim m_q^{-1}$; numerically large scalar nucleon expectation values $\chi_q \approx 5$; the factor m_p/f_π .

In this connection we wish to emphasize that the searches for T-invariance violation in the nuclear transitions

Table 1

Limits on phenomenological constants

	d_n	η
$i(\bar{u}\gamma_5 u)(\bar{u}u)$	$2 \cdot 10^{-4}$	$1 \cdot 10^{-3}$
$i(\bar{u}\gamma_5 t^a u)(\bar{u}t^a u)$	$1.5 \cdot 10^{-4}$	$3.5 \cdot 10^{-3}$
$i(\bar{d}\gamma_5 d)(\bar{d}d)$	$2.5 \cdot 10^{-4}$	$1 \cdot 10^{-3}$
$i(\bar{d}\gamma_5 t^a d)(\bar{d}t^a d)$	$4 \cdot 10^{-4}$	$4 \cdot 10^{-3}$
$i(\bar{d}\gamma_5 d)(\bar{u}u)$	$2 \cdot 10^{-4}{}^a$	$8 \cdot 10^{-4}$
$i(\bar{d}\gamma_5 t^a d)(\bar{u}t^a u)$	$1 \cdot 10^{-3}{}^a$	$3 \cdot 10^{-1}{}^a$
$\frac{1}{2}\epsilon_{\mu\nu\alpha\beta}(\bar{u}\sigma_{\mu\nu}u)(\bar{d}\sigma_{\alpha\beta}d)$	$3 \cdot 10^{-5}$	$4 \cdot 10^{-2}{}^b$
$\frac{1}{2}\epsilon_{\mu\nu\alpha\beta}(\bar{u}\sigma_{\mu\nu}t^a u)(\bar{d}\sigma_{\alpha\beta}t^a d)$	$2.5 \cdot 10^{-4}$	$4 \cdot 10^{-2}{}^b$
$m_P \bar{u}g\sigma_{\mu\nu}G_{\mu\nu}^a t^a \gamma_5 u$	$2 \cdot 10^{-5}{}^a$	$1 \cdot 10^{-5}$
$m_P \bar{d}g\sigma_{\mu\nu}G_{\mu\nu}^a t^a \gamma_5 d$	$1 \cdot 10^{-5}{}^a$	$1 \cdot 10^{-5}$

and in the neutron reactions even at the level of accuracy of P-violation experiments would be as informative as the neutron EDM search are. Remind that the limit (2) for the effective T-odd nucleon-nucleon interaction, actively used by us, is just at the level of the Fermi constant. It should be emphasized that at this level of accuracy the background correlations due to the final-state interaction are not so dangerous.

As far as atomic experiments are concerned it should be said that a considerable progress is expected in the near future in this field⁵. For example, the measurement of the ¹⁹⁹Hg atom EDM at the same level of accuracy as that attained for ¹²⁹Xe, due to larger charge of Hg nucleus would allow one to advance by an order of magnitude in the value of η and, therefore, of the constants k considered. In this case the atomic limits would get ahead for a lot of operators.

We wish, however, to point out the evident complementarity of the experiments discussed: it can be seen from Table 1 that there are operators for which the neutron limits will remain leading ones for a long time.

We are grateful to V.V.Flambaum, O.P.Sushkov and A.R.Zhitnitsky for valuable discussions.

References

1. J.H.Christenson, J.W.Cronin, V.L.Fitch, R.Turlay, Phys. Rev. Lett. **13**, 138 (1964).
2. I.S.Altarev et al., ZhETF Pisma **44**, 360 (1986).
3. O.P.Sushkov, V.V.Flambaum, I.B.Khriplovich, ZhETF **87**, 1521 (1984) (Sov. Phys. JETP **60**, 873 (1984)).
4. V.V.Flambaum, I.B.Khriplovich, O.P.Sushkov, Phys. Lett. **162B**, 213 (1985); Nucl. Phys. **A449**, 750 (1986).
5. T.G.Vold, F.J.Raab, B.Heckel, E.N.Fortson, Phys. Rev.

- Lett. 52, 2229 (1984).
6. G.W.Wang et al., Phys. Rev., C18, 476 (1978);
O.C.Kistner, Phys. Rev. Lett., 19, 872 (1967).
 7. J.L.Gimlett, H.E.Henrikson, N.K.Cheung, F.Boehm, Phys. Rev., C24, 620 (1981); C25, 1567 (1982).
 8. I.B.Khriplovich, A.R.Zhitnitsky, Phys. Lett., 109B, 490 (1982).
 9. V.M.Khatsymovsky, I.B.Khriplovich, A.S.Yelkhovsky, Preprint 87-28, Novosibirsk, 1987; submitted to Ann. Phys.

Additional notes

1. Recent experiment with the molecule TlF (D.Schropp, D.Cho, T.Vold, E.A.Hinds, Phys. Rev. Lett. 59, 991(1987)), if interpreted in terms of the parameter η , leads to the limit more stringent than (2) by a factor about 3 with the corresponding changes in the last column of Table 1.

2. Contrary to the recent claim (J.F.Donoghue, B.R.Holstein, M.J.Musolf, Phys. Lett. B196, 196 (1987)), nuclear electric dipole moment is enhanced considerably with respect to corresponding nucleon values in the Kobayashi-Maskawa model. Using for the parameter η in this model the value $5 \cdot 10^{-10}$ (see (13)), which is in accordance with the constraints of chiral symmetry, we get for nuclear EDM d the result $d/e \sim 10^{-30}$ cm. It is substantially larger than the neutron EDM d_n in the same model (see again (13)). By the way, the latter result for d_n obtained in ⁸ was in fact confirmed by B.McKellar et al. (preprint UM-P-87/28, July, 1987) contrary to the opposite claim by Donoghue et al.

STATUS OF THE BATES PARITY VIOLATION EXPERIMENT

S. Kowalski

Bates Linear Accelerator Center
Laboratory for Nuclear Science and Department of Physics,
Massachusetts Institute of Technology,
Cambridge, MA 02139 USA

ABSTRACT

An experiment designed to measure precisely the parity violating interference in the elastic scattering of longitudinally polarized electrons from ¹²C is under way at the Bates Accelerator Center. The experiment required the construction of a high intensity polarized injector whose successful operation has been demonstrated. Present efforts are aimed towards the understanding and control of sources of systematic errors and completion of the measurements.

INTRODUCTION

The standard SU₂xU₁ model of the electroweak interaction is one of the most successful theories in physics. The weak neutral current and the predictions for the W and Z masses have been verified. High precision experiments involving a variety of probes: deep inelastic scattering, νp elastic scattering, νe scattering, atomic parity violation, e^+e^- annihilation, and the W and Z mass measurements are all in impressive agreement with this theory. Taken together, the data yield $\sin^2\theta_w = 0.230 \pm .0048$ for the one free parameter in the model. These data span a range in momentum transfer covering ten orders of magnitude ($10^{-6} < q^2(\text{GeV}/c) < 10^4$). Present experimental motivations include tests of the standard model at the level of radiative corrections.

Although many neutral current phenomena have been observed, one of the early experiments which provided a crucial test of the W-S model was the SLAC/Yale measurement of parity violation in the deep